HOKKAIDO UNIVERSITY

Title	Soil CO_2 emissions and net primary production in agricultural plantations on tropical peat
Author(s)	NUR, WAKHID
Degree Grantor	北海道大学
Degree Name	博士(農学)
Dissertation Number	甲第14213号
Issue Date	2020-09-25
DOI	https://doi.org/10.14943/doctoral.k14213
Doc URL	https://hdl.handle.net/2115/96154
Type	doctoral thesis
File Information	Nur_Wakhi.pdf

Hokkaido University Collection of Scholarly and Academic Papers : HUSCAP

Soil CO_2 emissions and net primary production in agricultural plantations on tropical peat

(熱帯泥炭地の農業プランテーションにおける土壌 CO_2 放出量と純一次生産)

Hokkaido University Graduate School of Agriculture

Division of Environmental Resource Doctoral Course

Nur Wakhid

Advisor : Prof. Dr. Agr. Takashi Hirano

Co-advisors : Prof. Dr. Agr. Ryoji Sameshima
: Assoc. Prof. Dr. Tomomichi Kato

Date of Oral Examination : 30.07.2020
Date of Approval :

Abstract

Land conversion from tropical peat swamp forest to plantations potentially results in a large amount of carbon dioxide (CO_2) emissions through oxidative peat decomposition because of lowered groundwater level (GWL) by drainage. Moreover, the land conversion would decrease carbon (C) sequestration through net primary production (NPP) because of vegetation change. Two major agricultural land uses in Indonesia's tropical peatland over the past decade are oil palm and rubber plantations. However, field-based information on their C balance is still limited. The objectives of this study were (1) to investigate the seasonal variations in total soil respiration (SR) and peat decomposition (PD) in a rubber plantation and to determine the contribution of PD to total subsidence, (2) to quantify the above- and belowground NPP of mature oil palm plantations and determine how much CO_2 was emitted through pruned frond decomposition, (3) to quantify SR, PD and NPP of a young oil palm plantation, and (4) to finally summarize the C dynamics of agricultural plantations on tropical peat.

First, soil CO_2 efflux was measured monthly using a closed chamber system from December 2014 to December 2015, in a rubber plantation on peat soil in Central Kalimantan, Indonesia. SR and PD were separately quantified by trenching. Also, peat surface elevation was measured to determine annual subsidence. With GWL, SR showed a negative logarithmic relationship ($p < 0.01$), whereas PD showed strong negative linearity ($p < 0.001$). Using the significant relationships, annual SR and PD were calculated from hourly GWL data to be 32.9 ± 10.4 and 14.1 ± 2.14 Mg C ha^{-1} yr^{-1} (mean ± 1 standard deviation), respectively. From the PD and peat properties, annual subsidence only through peat oxidation was estimated at 1.50 cm yr^{-1}, which accounted for 25% of total subsidence (5.96 cm yr^{-1}) on average.

Second, above- and belowground NPP and CO_2 emission through pruned frond decomposition (LD_{frond}) were assessed in two different mature oil palm plantations established on peat, an industrial plantation in Riau and a smallholder plantation in Jambi, Sumatra, Indonesia from February 2018 to July 2019. Aboveground NPP (ANPP) arises from the production of trees, pruned fronds, fruit bunches, and understory vegetation, whereas belowground NPP (BNPP) consists of the production of coarse roots including trunk bases and fine roots. Annual total NPP (ANPP + BNPP) was 17.3 and 13.5 Mg C ha^{-1} yr^{-1}, in the industrial and smallholder plantations, respectively. ANPP accounted for 81 and 73% of total NPP in the industrial and smallholder plantations, respectively. Using a negative exponential equation

determined by the litter bag method, annual LD_{frond} was estimated to be 1.48 and 1.12 Mg C ha^{-1} yr^{-1}, respectively, in the industrial and smallholder plantations.

Third, soil CO_2 emissions and NPP were measured in a young oil palm plantation on peat soil in South Kalimantan, Indonesia from September 2018 to March 2020. SR and PD were separately quantified by measuring at near (SR) and far (PD) positions from tree bases. Total NPP was estimated at 10.9 Mg C ha^{-1} yr^{-1}, of which ANPP accounted for 78%. Annual SR and PD were 23.1 and 15.4 Mg C ha^{-1} yr^{-1}, respectively. Annual subsidence through peat oxidation was 2.33 cm yr^{-1}, which accounted for 14% of total subsidence (17.2 cm yr^{-1}). Annual CO_2 emission through pruned frond decomposition (LD_{frond}) was estimated to be 0.38 Mg C ha^{-1} yr^{-1}. Therefore, heterotrophic respiration (HR) as a sum of PD and LD_{frond} was 15.8 Mg C ha^{-1} yr^{-1}, resulting in a net C source of 4.9 Mg C ha^{-1} yr^{-1} (= NPP – HR).

Comparable PD (14.1 and 15.4 Mg C ha^{-1} yr^{-1}) at similar mean GWL (-0.69 and -0.74 m), in rubber and young oil palm plantations, indicates that GWL can be used as a proxy for peat decomposition even at different land uses. Besides tree age, plantation management significantly affected NPP. A young oil palm plantation in South Kalimantan was a CO_2 source, resulting from lower NPP due to immaturity.

Acknowledgements

First and foremost, I owe an immense gratitude of thanks to my supervisor, Prof. Takashi Hirano, for his constant advice, guidance, patience, and support during my study from Master to Ph.D.

I would like to acknowledge and deepest appreciation to the reviewers of my thesis, Prof. Ryoji Sameshima and Dr. Tomomichi Kato for their valuable comments and suggestions.

I would like to express my sincere appreciation to Indonesian Agency for Agricultural Research and Development, for this a great opportunity to continue the study and granting me the scholarship. Without their support it would not be possible for me to continue my study in Japan.

I would also like to thank Dr. Hiroyuki Yamada and Dr. Okada Keiji for their valuable comments during my study.

I would like to thank all the laboratory member of Ecological and Environmental Physics, Graduate School of Agriculture, for their friendly company and support during my stay in Japan. Great acknowledgment is given to all Indonesian students, Samurai and sholawat group, for their support and help me with a wonderful Japanese life experience. All these experiences are priceless and will always be remembered.

Special thanks to my colleague in Indonesia, Prof. Fahmuddin Agus, Dr. Ai Dariah, Husni and his staff, Udin, and Zainudin, for their collaboration and supporting the field research in Indonesia.

I would also like to extent my deepest appreciation to Prof. Dedi Nursyamsi for his continuous support since Master to Doctoral degree in Japan.

I would like to gratefully thank all my colleague in Indonesian Swampland Agricultural Research Institute, for a lot of support during my study.

Lastly, words fail me to express my appreciation to my parents, my family, Intan Sulistiowati, Muhammad Ilham, Muhammad Fatih Rajab, and Farayaka Khadijah for their love and persistent confidence in me.

Contents

Abstract ..... **iii**

Acknowledgements ..... **v**

Chapter 1. Introduction **1**
1.1. Background 1
1.2. Objectives 4

Chapter 2. Soil CO_2 emissions from a rubber plantation on tropical peat in Central Kalimantan **5**
2.1. Material and methods 5
2.1.1. Study site 5
2.1.2. Experimental design 5
2.1.3. Soil CO_2 efflux measurement 7
2.1.4. Subsidence 8
2.1.5. Peat properties 8
2.1.6. Soil environment 9
2.1.7. Conversion of peat decomposition to subsidence 9
2.1.8. Statistical analysis 9
2.2. Results 9
2.2.1. Seasonal variations in groundwater level and soil temperature 9
2.2.2. Seasonal variations in soil CO_2 efflux 10
2.2.3. Relationships of soil CO_2 efflux with soil environmental factors 11
2.2.4. Annual CO_2 emissions 13
2.2.5. Contribution of peat decomposition to total subsidence 14
2.3. Discussion 17
2.3.1. Controls on soil CO_2 efflux 17
2.3.2. Annual CO_2 emissions 19
2.3.3. Contribution of peat decomposition to total subsidence 21

Chapter 3. Net primary production and CO_2 emission through frond decomposition in oil palm plantations on peat in Sumatra **23**
3.1. Material and methods 23
3.1.1. Study site 23
3.1.2. Above- and belowground net primary production 24

3.1.3. Litter/ frond decomposition 26
3.1.4. Data analysis 27
3.2. Results 27
3.2.1. Characteristic of oil palm component 27
3.2.2. Aboveground and belowground net primary production (ANPP and BNPP) 28
3.2.3. CO_2 emission through pruned frond decomposition 29
3.3. Discussion 36
3.3.1. ANPP (including understory) 36
3.3.2. BNPP (including fine root dynamics) 37
3.3.3. Pruned frond decomposition 38
3.3.4. Comparison with other oil palm plantations and tropical ecosystems 39

Chapter 4. Soil CO_2 emissions and net primary production (NPP) of an oil palm plantation on peat in South Kalimantan 41
4.1. Material and methods 41
4.1.1. Study site 41
4.1.2. Soil CO_2 efflux measurement 41
4.1.3. Litter/ frond decomposition 42
4.1.4. Net primary production (NPP) 43
4.1.5. Soil environment 44
4.1.6. Statistical analysis 45
4.2. Results 45
4.2.1. Oil palm component characteristic 45
4.2.2. Soil environmental factors 45
4.2.3. Soil CO_2 efflux 47
4.2.4. Peat subsidence 50
4.2.5. CO_2 emission through pruned frond decomposition (LD_{frond}) 52
4.2.6. Net primary production (NPP) 53
4.3. Discussion 56
4.3.1. Soil CO_2 emissions 56
4.3.2. Litter decomposition (LD) and total soil respiration (SR_{tot}) 58
4.3.3. Net primary production (NPP) 59
4.3.4. Carbon (C) emission through heterotrophic respiration (HR) versus C sequestration through net primary production (NPP) 60

Chapter 5. General discussion 61
5.1. Soil CO_2 emissions including litter decomposition of agricultural plantations on peat soil 61
5.2. Carbon sequestration through net primary production (NPP)..... 62
5.3. Carbon balance of agricultural plantations on peat soil 62
5.4. Implications for tropical peat management..... 63

Chapter 6. Conclusions..... 65

References..... 67

Chapter 1. Introduction

1.1. Background

Tropical peat soil has stored a huge amount of carbon in thick layers as a result of organic matter accumulation over thousands of years under a water-logged condition. Despite covering only 11% of global peatland areas, tropical peatlands contain about 88.6 Gt (15–19% of the global peat carbon (C) pool), of which 77% were distributed in Southeast Asia (Page et al., 2011a). Indonesia has the largest area of tropical peatlands, which covers 2.48×10^7 ha and stores 68.5 Gt of carbon mainly in Sumatra, Kalimantan, and Papua Islands (Page et al., 2011a; Wahyunto et al., 2014). However, during the last two decades, this carbon-rich ecosystem has been threatened by deforestation and drainage (Afriyanti et al., 2016). Also, the high demand for plantations has increased land clearing on tropical peatlands (Miettinen et al., 2012). In Malay Peninsula, Sumatra, and Borneo, peat swamp forest has decreased from 41% to 29% of total peat area over the period mainly for agricultural and plantation purposes (Koh et al., 2011; Miettinen et al., 2016). Land-use change in peatland is usually related to large carbon dioxide (CO_2) emissions due chiefly to drainage, which lowers groundwater level (GWL) and disturbs the peat soil condition (Furukawa et al., 2005; Couwenberg et al., 2009). Thus, land-use change potentially changes peatland from an important carbon sink into a huge source of CO_2 to the atmosphere and increases fire risks (Page et al., 2002; Page et al., 2011b; Agus et al., 2013; Schrier-Uijl et al., 2013).

Two major agricultural land uses in Indonesia's tropical peatland during the past several years are oil palm and rubber plantations. Oil palm (*Elaeis guineensis*) plantations has become global attention in recent years for their fast development due to high demand for their products in the world. In Southeast Asia, oil palm plantations and their expansion are suspected as a driver of deforestation, including on tropical peat swamp forest in Indonesia (Carlson et al., 2012; Kharina et al., 2016; Pirker et al., 2016). The proportion of peat swamp forests in Sumatra and Kalimantan fell from 76% in 1990, to 40% in 2007 and 29% in 2015, of which mostly the newly established plantations are oil palm (Miettinen et al., 2016). Recently, oil palm plantations became the most common agricultural land use in Indonesia, the largest palm oil-producing country in the world (FAOSTAT, 2014). The total area of oil palm plantations on peat soil increased from 0.42 Mha in 1990 to 2.43 Mha by 2010 in Indonesia and Malaysia (Gunarso et al., 2013).

Another fast-expanding plantation crop in the last three decades is rubber. Indonesia is the world's second largest natural rubber exporter after Thailand, with the largest area of rubber plantations in the world (Global Business Guide Indonesia, 2015). Rubber plantations which occupy about 3.6 million ha are the second largest plantation in Indonesia after oil palm plantation (BPS-Statistics Indonesia, 2019). Also, the second largest in the production and export value of total Indonesian plantation commodities after oil palm. On peat soil, although the area of rubber plantation is still limited in comparison with those of oil palm plantation, rubber plantations have been expanding year by year. Thus, the impact of the peat land use conversion into rubber plantations is also important.

Carbon balance of tropical peatland plays an important role in the global carbon cycle. Therefore, recently, study of tropical peatland C dynamics is of concern to peat scientist. For C emission, several studies of soil CO_2 emission were conducted on tropical peatland, however, few of them quantify oxidative peat decomposition or heterotrophic respiration from total soil respiration separately (Jaiuhainen et al., 2012; Melling et al., 2013; Itoh et al., 2017; Ishikura et al., 2018). Total soil respiration (SR) consists of the autotrophic or root respiration (RR), oxidative peat decomposition (PD), and litter decomposition (LD) components. The two-latter component usually defined as heterotrophic respiration (HR). Of several methods, typically, peat soil CO_2 emissions have been assessed using two methods: the subsidence and chamber methods. The subsidence method measures the relative elevation of peat surface along with C content and bulk density (BD) of peat. On the other hand, the chamber method directly measures CO_2 emission rates (efflux) from peat soil surface.

The subsidence method has an advantage as backwards interpretation of soil carbon loss. The thickness of peat layer reduces because of compaction, shrinkage, consolidation, and oxidative peat decomposition which releases CO_2 to the atmosphere. The principal question of the method is how to determine the resultant extent of peat oxidation (Hooijer et al., 2010). Even if many researchers have attempted to determine the contribution of peat decomposition to total subsidence, it is still unclear. The role of peat oxidation in subsidence of the drained peat layers has not been sufficiently quantified yet (Couwenberg et al., 2009). As for the chamber method, there are several studies in agricultural land uses on tropical peat (e.g. Melling et al., 2005; Ali et al., 2006; Jauhiainen et al., 2012; Marwanto and Agus, 2014; Melling et al., 2013; Husnain et al., 2014). However, only small number of studies that measured PD directly in the field (Jauhiainen et al., 2012; Dariah et al., 2014; Husnain et al., 2014; Melling et al., 2013; Hergoualc'h et al., 2017; Ishikura et al., 2018; Manning et al., 2019). The direct measurement of soil CO_2 emission, excluding RR, is critical to quantify CO_2 emissions

arising solely from PD. Moreover, to reduce uncertainties in the assessment of peat CO_2 emissions, it is indispensable to understand the variability of PD with environmental factors.

In recent years, closed chamber system using trenching method is widely applied to separate SR into PD and RR in forest or plantations (Melling et al., 2013; Comeau et al., 2016; Itoh et al., 2017; Hergoualc'h et al., 2017; Ishikura et al., 2018). However, in oil palm plantations, PD can be measured separately free from RR contribution in far position from the tree base because root distribution of oil palm tree was declined with the distance from the tree base (Dariah et al., 2014; Manning et al., 2019). Additionally, in oil palm plantation, different management area i.e. 1) frond stack (FS), inter row for pruned fronds heap which are usually rich with organic material, and 2) harvesting path (HP), subject of compaction, also supposed to have different contribution to the soil CO_2 emission.

There are several publications on PD or HR in oil palm plantations on peat soil (e.g. Melling et al., 2013; Dariah et al., 2014; Ishikura et al., 2018). However, none of these have studied CO_2 emission through palm litter (pruned fronds) decomposition (LD_{frond}). Pruned fronds of oil palm trees break down mostly into CO_2, followed by dissolved organic carbon (DOC), organic or inorganic nutrients, and stable humus (Bragazza et al., 2008). As far as we are aware, there are no data of CO_2 emissions through frond decomposition in oil palm plantations on tropical peat. Given that pruned frond decomposition continuously releases CO_2, field experiments are necessary to understand the contribution of LD_{frond} to the carbon balance of oil palm plantations on peat soil.

Along with C emission, the conversion of peat swamp forest to plantations potentially decreases carbon sequestration through lowered photosynthesis and would decrease net primary production. However, C sequestration through net primary production (NPP), particularly from oil palm plantation on peat soil remained poorly investigated. Most of the published studies focus on forest biomass (Yuan and Chen, 2012; An et al., 2017), while the study of total above and belowground biomass production (NPP) in oil palm plantation has seldom been conducted (Kotowska et al., 2015). NPP is an essential component of carbon and nutrient cycles in terrestrial ecosystems. However, there are still a limited number of studies on the NPP of oil palm plantations (Melling et al., 2008; Tan et al., 2014; Kotowska et al., 2015; Basuki et al., 2018), and only two studies were reported the NPP of oil palm plantations established on peat soil (Melling et al., 2008; Basuki et al., 2018), though these were conducted in young plantations (2-5 years old), and some parts of NPP, such as fine root production, were not measured directly. Thus, to our knowledge, there is no field

information on above- and belowground NPP in mature oil palm plantations on peat soil.

1.2. Objectives

This study investigated the C dynamics of two main agricultural plantations in Indonesia's tropical peatland, oil palm and rubber plantations, by quantifying C sequestration through NPP and soil CO_2 emissions separately. Both NPP and soil CO_2 emissions are important information to understand the carbon balance of oil palm and rubber plantation ecosystems. Our detailed research objectives were separated into several chapters below.

1. To investigate the seasonal variations of SR and PD separately in a rubber plantation on tropical peat and to determine the contribution of oxidative peat decomposition to total subsidence, using the year-round field data (Chapter 2).
2. To quantify the above and belowground NPP of mature oil palm plantations established on peat and determine how much CO_2 is emitted through the decomposition of pruned fronds left on the ground (Chapter 3).
3. To estimate two contrast fluxes, the annual soil CO_2 emissions and C sequestration through NPP of a young oil palm plantation on deep tropical peat (Chapter 4).

Chapter 2. Soil CO_2 emissions from a rubber plantation on tropical peat in Central Kalimantan

2.1. Material and methods

2.1.1. Study site

A rubber (*Hevea brasiliensis*) plantation was established on peat soil in Central Kalimantan, Indonesia (02°29′50″S, 114°11′20″E). The peat depth was 5 m on average. The study site was originally a peat swamp forest but was deforested and drained through the large-scale land development called Mega Rice Project (MRP) in the late 1990s. The site was abandoned after MRP and burnt by wild peat fire in El Niño years. In 2007, rubber trees were planted for latex harvest at intervals of 3 and 6.5 m with intercropping pineapple plants between tree rows after peat compaction using heavy machinery. The age of rubber trees was eight years old and the tree height was approximately 6 m in 2015. Rubber trees defoliated in the dry season from June to November, which resulted in a large accumulation of leaf litter on the ground. A combination of chemical and organic (manure) fertilizers was applied in the first two years at a rate of 1.5 ton yr^{-1} ha^{-1}, which was equivalent to 185 kg N ha^{-1}, 185 kg P_2O_5 ha^{-1}, 183 kg K_2O ha^{-1} and 120 kg S ha^{-1}, by piling up the fertilizer at tree bases. For the top 0.75-m-thick peat, bulk density (BD) was 0.23 g cm^{-3}, C and nitrogen (N) contents were 42.8% and 2.34%, respectively, and consequently the C/N ratio was 18.3. Mineral content showed an increase tendency below 0.5 m (detailed in Table 2). For the top 0.5-m-thick peat, pH was 3.4 and 3.5, respectively, in the dry and wet seasons (personal communication).

2.1.2. Experimental design

Soil CO_2 efflux was measured in rubber plantation on peat soil in Central Kalimantan, Indonesia, from December 2014 to December 2015. A strong El Niño event occurred in the period (Schiermeier, 2015). To exclude root respiration and directly measure CO_2 efflux through peat decomposition (PD), three trenching plots with a respective area of 1 × 1 m^2 were established in June 2014, which were about 40 m distant from a drainage canal (Fig. 1). We began flux measurement six months after trenching, waiting for the calming of extra CO_2 emissions through the decomposition of dead roots produced by trenching (Epron, 2009). Each plot was trenched 1 m deep into peat to cut roots, and then four plastic plates were inserted in trenches to prevent roots from invading into the plot. After trenching, four chamber bases were installed in each plot to avoid disturbing the peat surface when a chamber is set. For total soil

respiration (SR), 12 chamber bases were distributed outside of the trenching plots. Tree roots are relatively localized around each tree, and root respiration depended on the distance from trees in an acacia plantation (Jauhiainen et al., 2012). Thus, the 12 chamber bases were aligned between tree rows with the same distance and categorized into two groups (near (1.5 m) and far (3 m) positions) by the distance from rubber trees to examine the difference of root respiration (Figs. 1 and 2). The depth of insertion into peat soil was 3 cm in all chamber bases. SR reflects a combination of PD, root respiration (RR) and the decomposition of leaf litter (LD).

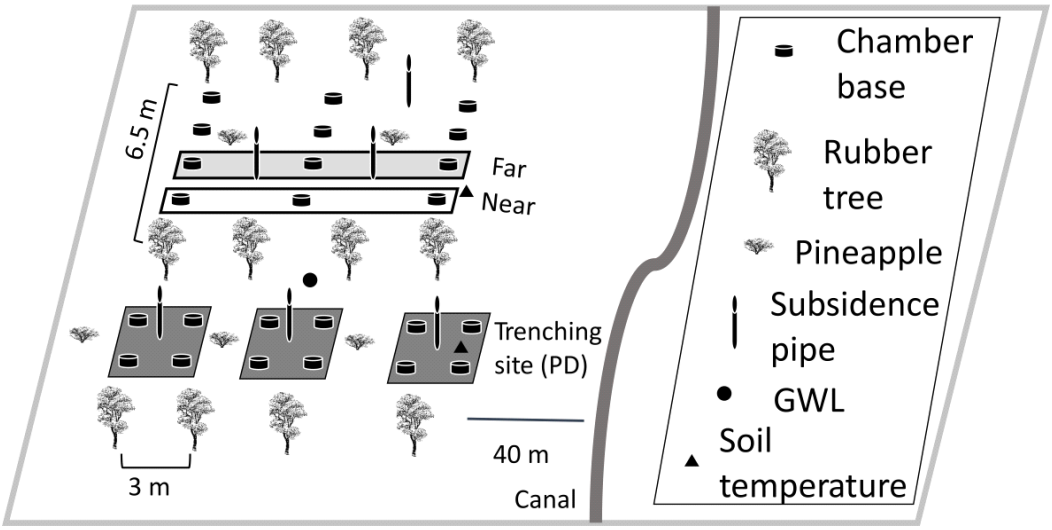

Fig. 1. Experimental plots and the distribution of chamber bases and ground sensors in Central Kalimantan.

Fig. 2. Experimental scenes of (a) peat decomposition (PD) and (b) total soil respiration (SR).

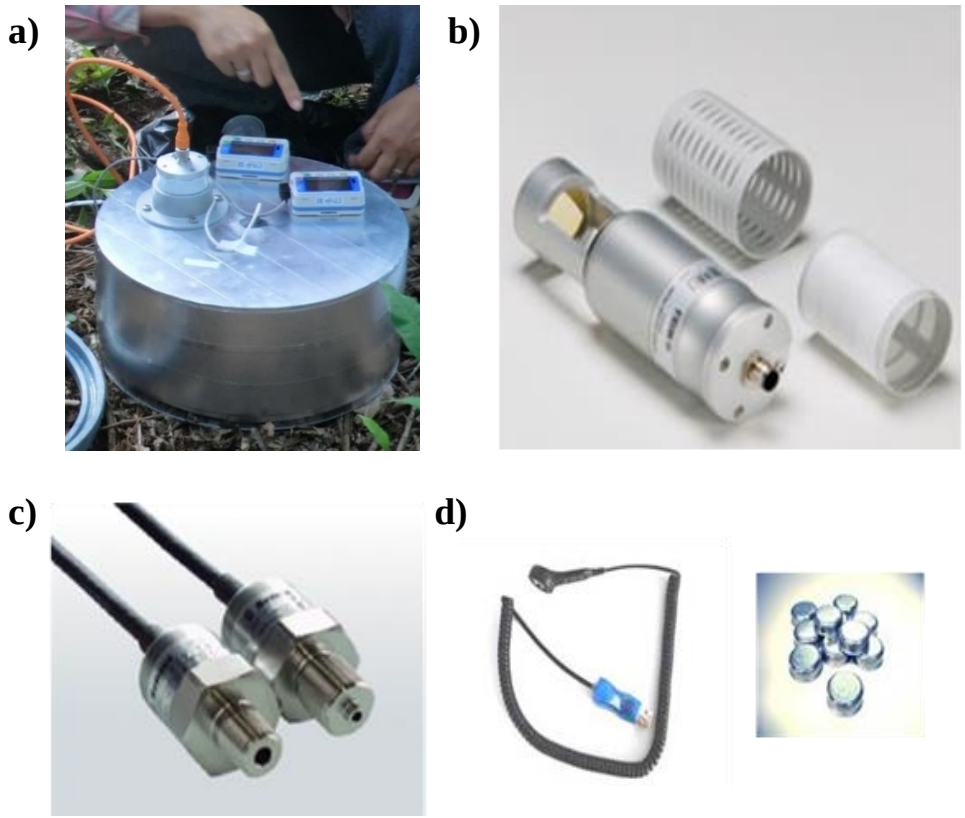

Fig. 3. Instruments for CO_2 emission and environmental factor measurement, (a) closed chamber system, (b) portable infrared CO_2 analyzer, (c) GWL sensor, and (d) soil temperature sensor.

2.1.3. Soil CO_2 efflux measurement

Soil CO_2 efflux (PD and SR) was measured monthly on chamber bases using a closed chamber system, to which a portable infrared CO_2 analyzer (GMP343, Vaisala, Helsinki, Finland), DC voltage data logger (LR 5042, HIOKI, Nagano, Japan) and temperature data logger (LR5011, HIOKI) were installed (Fig. 3). A chamber made of opaque PVC with 30 cm in diameter and 20 cm in height was employed. The gas analyzer was calibrated every six months using standard gases. Throughout the study period, all plants were picked out from trenching plots, though understory plants were few in the plantation. Before measurement, leaf litter was removed from chamber bases in the trenching plots to exclude CO_2 emissions through litter decomposition. The chamber and base were water-sealed after the chamber was ventilated using a fan.

Air temperature and CO_2 concentration in chamber headspace were measured every 10 seconds for three minutes on each chamber base. Simultaneously, soil

temperature was measured at a depth of 5 cm using a digital thermometer near chamber bases. To cover a considerable temperature range, the measurement was replicated three times a day (8:30-10:30, 11:30-13:30 and 14:30-16:30). Soil CO_2 efflux (μmol m^{-2} s^{-1}) was calculated from air temperature (T_a, ºC) and an increasing rate of CO_2 concentration (*dC/dt*, μmol mol^{-1} s^{-1}) using the following equation:

$$CO_2 \text{ efflux} = \left(\frac{dC}{dt}\right).\left(V/\left(V'(273.2 + T_a)/273.2\right)\right)/A \quad (1)$$

where *V* is chamber volume (0.0144 m^3), *V'* is molar volume of air at 0°C (0.0224 m^3 mol^{-1}) and *A* is covered ground area by the chamber (0.0707 m^2). *dC/dt* was determined from CO_2 concentrations during the last two minutes of measurement using the least-square method.

A linearity test was applied to control the quality of *dC/dt* following Aguilos et al. (2013). Also, relative humidity was measured in the headspace with a small hygrometer (SHTDA-2, SysCom Inc., Tokyo, Japan) to quantify the effect of water vapor dilution on CO_2 concentration (Harazono et al., 2015; Matsuura et al., 2011).

2.1.4. Subsidence

Ground subsidence was determined from temporal change in peat surface elevation, which was measured simultaneously with the flux measurement using steel pipes inserted vertically into peat and anchored firmly at underlying mineral substrate. Three steel pipes were installed in the inside and outside of the trenching, respectively (Figs. 1and 2).

2.1.5. Peat properties

To analyze bulk density (BD) and C content, five peat samples were collected, respectively, at six depths from 0 to 75 cm in the dry season (September 2014) when GWL was low. Peat samples were taken horizontally from a pit using 100-cm^3-large core samplers to keep the sample from compression (Hooijer et al., 2012). The pit was excavated in the middle of rubber trees, where root density was expected to be minimal. Peat BD was determined in a laboratory by a gravimetric method. Carbon content was determined using a CN analyzer (CNS-2000 elemental analyzer, LECO Corporation, Michigan, USA).

2.1.6. Soil environment

Groundwater level (GWL), which was defined as the relative elevation of the groundwater surface to the ground surface, was measured hourly using a water pressure sensor (Model HTV 050KP-10-V, Sensez Co., Tokyo, Japan) in a perforated PVC pipe inserted vertically deep into mineral soil. Soil temperature was recorded hourly using a temperature data logger (Thermochron SL type, KN laboratories, Osaka, Japan) installed at a depth of 5 cm both inside and outside of the trenching (Fig. 1).

2.1.7. Conversion of peat decomposition to subsidence

The annual PD (gC m^{-2} y^{-1}) was converted to corresponding subsidence (PDs, cm y^{-1}) using BD (g cm^{-3}) and carbon content (CC, % in mass) using the following equation (Agus et al., 2011):

$$PDs = PD/BD/CC/100 \quad (2)$$

2.1.8. Statistical analysis

One-way ANOVA and Pearson correlation analysis were conducted using R software (R Development Core Team 2015; version 3.1.3).

2.2. Results

2.2.1. Seasonal variations in groundwater level and soil temperature

During the flux measurement period from December 2014 to 2015, the dry season, which is commonly defined as months with monthly precipitation <100 mm (Hirano et al., 2015), lasted for four months from July through October (Fig. 4a). In particular, monthly precipitation was <5 mm in August and September. In spite of an El Niño drought, annual precipitation measured 2506 mm yr^{-1}, which was almost identical to the 14-year-long mean between 2002 and 2015 (2553 ± 465 mm yr^{-1}; mean ± 1 standard deviation (SD)).

Mean annual GWL was -0.69 m during the flux measurement period. GWL varied seasonally between -1.71 and 0.03 m (Fig. 4b). GWL was high in the wet season from December to May and low in the dry season from June to November following a seasonal variation in precipitation (Fig. 4a). In 2015, the minimum GWL was lower at -1.71 m than in 2014 at -1.35 m because of the prolonged dry season due to a strong El Nino event (Schiermeier, 2015). Mean daily soil temperature ranged between 25 and 28 °C during the flux measurement period. Mean annual soil temperatures inside and outside the trenching were 26.4 and 26.9 °C, respectively, with no significant

difference ($p > 0.05$, Fig. 4c). Soil temperature showed a positive linearity with GWL ($p < 0.05$) in spite of low r^2 both inside and outside the trenching.

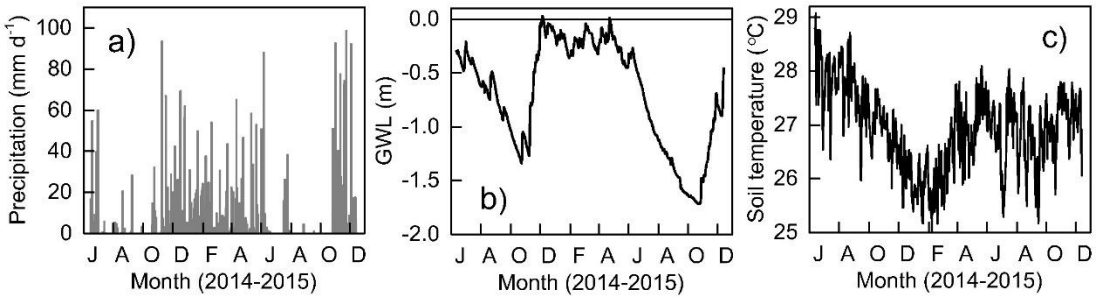

Fig. 4. Variations in daily values of (a) precipitation, (b) groundwater level (GWL) and (c) soil temperature inside (black) and outside (grey) the trenching from June 2014 to December 2015. Precipitation was measured in Palangkaraya (Hirano et al., 2009), which was about 25 km distant from the study site.

2.2.2. Seasonal variations in soil CO_2 efflux

PD showed a large seasonal variation and a negative correlation with GWL (Figs. 4b and 5a); PD increased up to about 10 g C m^{-2} d^{-1} in the dry season and remained low at 0–2 g C m^{-2} d^{-1} during the wet season. Although GWL was lowest in late October 2015 (Fig. 4b), the highest PD was measured in November, just after the first considerable precipitation event in the coming wet season (Fig. 5a). In contrast, seasonal variation in SR was small after February (Fig. 5b). PD averaged at 3.98 ± 0.39 g C m^{-2} d^{-1} (±1 standard deviation (SD), $n = 3$), whereas SR averaged at 8.61 ± 2.92 and 8.19 ± 2.16 g C m^{-2} d^{-1}, respectively, at near and far positions ($n = 6$); the two means of SR were not significantly different ($p > 0.05$). The residual between the means of SR and PD showed a different seasonal variation, which increased in the wet season (Fig. 5c).

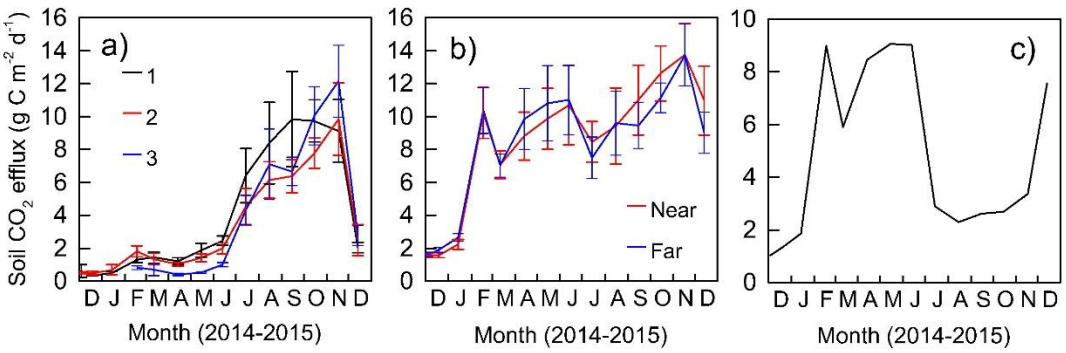

Fig. 5. Seasonal variations in daily mean (a) peat decomposition (PD, three trenching plots, n = 4), (b) total soil respiration (SR, near and far positions from tree rows, n = 6) and (c) residual between means of SR and PD from December 2014 to December 2015. Vertical bars in (a) and (b) denote 1 standard error (SE).

2.2.3. Relationships of soil CO_2 efflux with soil environmental factors

The relationship between PD and soil temperature was not significant (p > 0.05), whereas SR showed significant positive correlation with soil temperature (p < 0.05), but r^2 was low at 0.15 (Fig. 6). On the other hand, although PD increased linearly as GWL lowered (p < 0.001, Fig. 7), SR increased logarithmically with GWL lowering both at near and far position (p < 0.01, Fig. 8). The regression for PD and SR, was improved when the data in November 2015 were excluded, because the data were most probably pulse-like instantaneous CO_2 efflux and were caused by a considerable amount of rain at the beginning of the wet season after a severe drought (Lee et al., 2004). If daily data are averaged within the three plots, correlation is expressed as PD (g C m^{-2} d^{-1}) = -0.04 - 5.40 × GWL (m) (r^2 = 0.99). This equation suggests that every lowering of GWL by 0.1 m causes additional PD of 0.54 g C m^{-2} d^{-1}, and PD becomes almost zero when GWL rises up to 0 m.

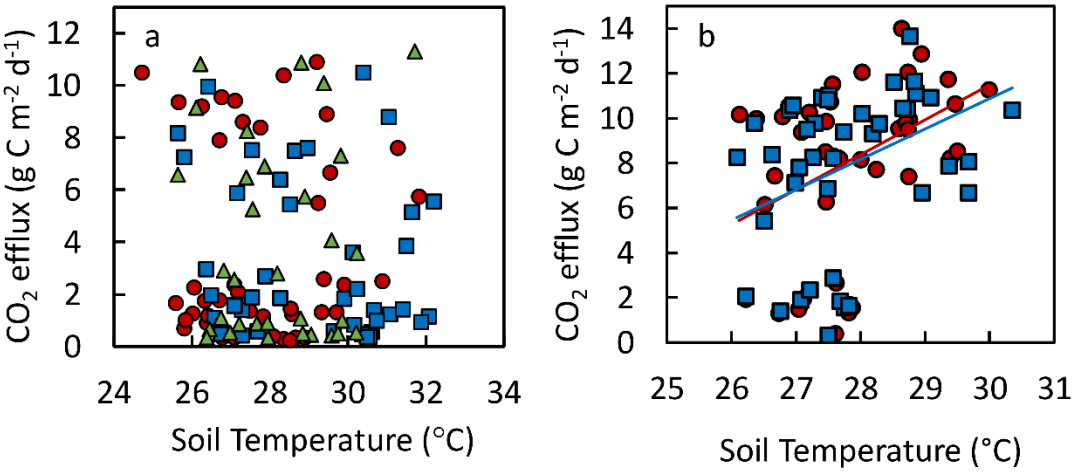

Fig. 6. Relationship between (a) peat decomposition (PD) and soil temperature in trenching 1 (circles), 2 (squares) and 3 (triangles), (b) total soil respiration (SR) and soil temperature for near (circles) and far (squares) positions from tree rows. Each symbol denotes one chamber base. A line is fitted for SR ($p < 0.05$) at near ($y = 1.56x - 35.2$; $r^2 = 0.15$) and far ($y = 1.35x - 29.8$; $r^2 = 0.14$) positions from rubber tree.

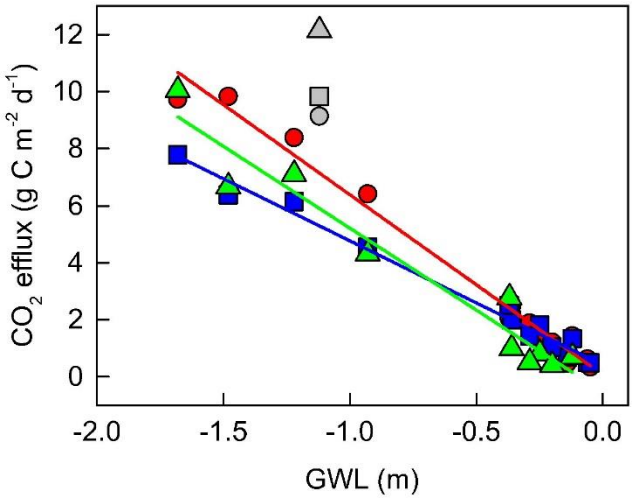

Fig. 7. Relationship between peat decomposition (PD) and groundwater level (GWL) in trenching 1 (circles), 2 (squares) and 3 (triangles). Each symbol denotes a daily average ($n = 4$). A grey symbol denotes November's measurement. A line is fitted without the grey symbol for each trenching ($p < 0.001$): 1) $y = 0.07 - 6.3x$ ($r^2 = 0.98$), 2) $y = 0.41 - 4.35x$ ($r^2 = 0.98$), 3) $y = -0.53 - 5.74x$ ($r^2 = 0.94$).

2.2.4. Annual CO_2 emissions

Annual soil CO_2 emissions (g C m^{-2} yr^{-1}) from December 2014 to December 2015 were calculated from hourly GWL data (Fig. 4b) for each trenching plot (PD) and chamber base (SR), respectively, using the linear (Fig. 7) or logarithmic (Fig. 8) relationships; data in November 2015 were excluded. Also, mean annual soil CO_2 efflux (g C m^{-2} d^{-1}), including the November's data, was simply converted into annual CO_2 emissions (Table 1). Annual CO_2 emissions of PD were 1408 ± 214 and 1454 ± 144 g C m^{-2} yr^{-1}, whereas those of SR were 3293 ± 1039 and 3068 ± 899 g C m^{-2} yr^{-1}. There was no significant difference between the two methods ($p > 0.05$) both for PD and SR. SR was not significantly different between near and far positions from tree rows ($p > 0.05$). On the other hand, we confirmed that SR was significantly larger than PD ($p < 0.001$). The residual of SR from PD was 1614–1885 g C m^{-2} yr^{-1}, which corresponds to the annual sum of root respiration (RR) and leaf litter decomposition (LD). PD accounted for 43–47% of SR on an annual basis.

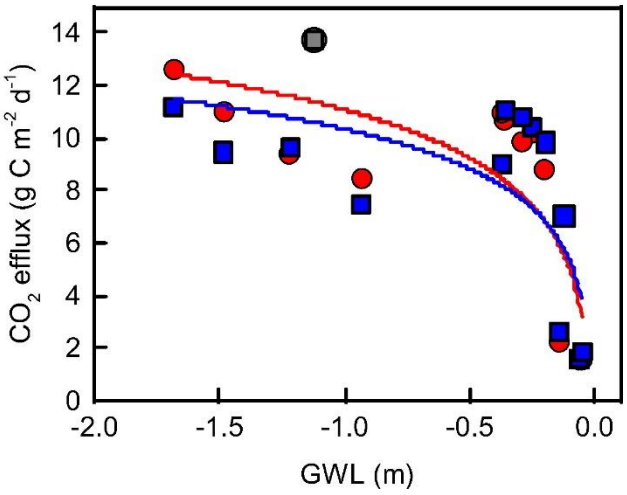

Fig. 8. Relationship between total soil respiration (SR) and groundwater level (GWL) for near (circles) and far (squares) positions from tree rows. Each symbol denotes a daily average ($n = 6$). A grey symbol denotes November's measurement. A logarithmic curve is fitted without the grey symbol for each position ($p < 0.01$): near) $y = 11.1 - 2.63.\ln(-x)$ ($r^2 = 0.61$), far) $y = 10.4 - 2.17 \ln(-x)$ ($r^2 = 0.47$).

Table 1. Annual CO_2 emissions estimated using two methods (mean ± 1 SD).

Treatment	Annual CO_2 emissions from groundwater level (g C m^{-2} yr^{-1})	Annual CO_2 emissions from mean efflux (g C m^{-2} yr^{-1})
PD		
Trenching 1	1655	1556
Trenching 2	1278	1290
Trenching 3	1289	1516
Mean (n = 3) (a)	1408 ± 214	1454 ± 144
SR		
Near position (n = 6)	3398 ± 1266	3144± 1068
Far position (n = 6)	3187 ± 864	2991± 788
Mean (n = 12) (b)	3293 ± 1039	3068 ± 899
Residual (b – a)	1885	1614

2.2.5. Contribution of peat decomposition to total subsidence

Elevation of the peat surface basically varied in parallel to GWL (Fig. 9) with a significant positive relationship ($p < 0.001$), though it showed a hysteresis (data not shown). Even at the same GWL, the elevation was higher in the early dry season when GWL was lowering than in the early wet season when GWL was rising. The hysteresis reflects oxidative peat decomposition during the dry season with low GWL, leading to irreversible subsidence. Peat surface elevation relative to the initial value in June 2014 was 0.72 ± 0.72 and -0.20 ± 1.19 cm (mean ± 1 SD, n = 3) for outside and inside trenching, respectively, on December 4, 2014, and -8.11 ± 3.51 and -8.99 ± 1.11 cm, respectively, on December 13, 2015. As the difference in elevation, annual subsidence was calculated to be 8.61 ± 3.20 and 8.58 ± 0.43 cm yr^{-1}, respectively, for outside and inside trenching after adjusting the number of days (from 374 to 365 days). However, the annual subsidence was most likely overestimated, because GWL was higher by 0.31 m on December 4, 2014 (-0.06 m) than on December 13, 2015 (-0.37 m). Lower GWL potentially results in lower elevation independently of peat decomposition. Thus, the measured elevation on the initial day was linearly interpolated for GWL of -0.37 m. The sensitivities of elevation to GWL, which were calculated from three consecutive data from mid-November to mid-December 2014, were 10.0 and 8.8 cm m^{-1}, respectively, for outside and inside trenching. As a result, the corrected annual rates of subsidence were 5.64 ± 3.20 and 5.96 ± 0.43 cm yr^{-1} for outside and inside trenching, respectively; the corrected annual subsidence was 5.36, 6.29 and 6.24 cm yr^{-1}, respectively, in the trenching 1, 2 and 3. There was no significant difference in annual subsidence between inside and outside ($p > 0.05$). To quantify the contribution of oxidative peat decomposition to the subsidence, firstly, annual PD estimated from hourly GWL (1408 ± 214 g C m^{-2} yr^{-1}) (Table 1) was converted to subsidence using

BD and carbon content of peat at different depths (Table 2), based on a simple assumption that the peat oxidation occurred only at each depth. Because BD and carbon content varied vertically, subsidence through PD ranged from 1.13–1.18 cm yr^{-1} at depth of 10–25 cm to 1.92 cm yr^{-1} in the top layer (0–5 cm). The PD subsidence averaged at 1.50 cm yr^{-1} and accounted for 25% of total subsidence inside trenching (5.96 cm yr^{-1}) on average.

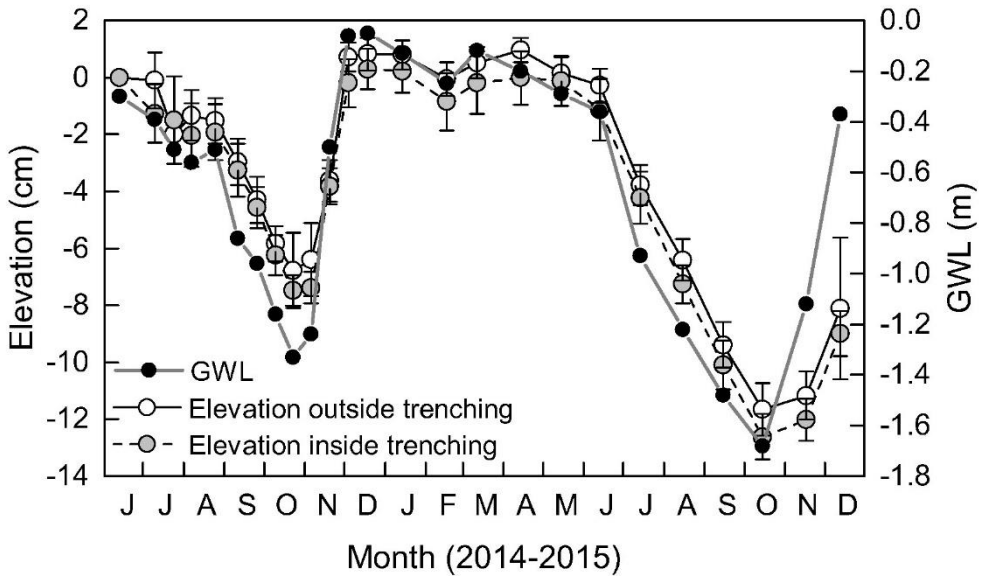

Fig. 9. Seasonal variations in peat surface elevation and groundwater level (GWL) from June 2014 through December 2015. Mean elevation (n = 3) is shown relatively to that in June 2014. Vertical bars denote 1 standard deviation.

Table 2. Peat properties and annual subsidence through oxidative peat decomposition (PD). Annual PD estimated from hourly groundwater levels (GWL) was converted to annual subsidence using bulk density (BD) and carbon content of peat at different depths. For BD and soil water content, mean ± 1 SD (n = 5) is shown at each peat depth. For PD, subsidence through PD and total subsidence, mean ± 1 SD of three trenched plots are shown. Peat samples were collected in September 2014, when GWL was −0.88 m.

Annual PD (g C m^{-2} yr^{-1})	Peat depth (cm)	BD (g cm^{-3})	Carbon content (%)	Nitrogen content (%)	Sulfur content (%)	Soil water content (m^3 m^{-3})	Subsidence through PD (cm yr^{-1})	Total subsidence (cm yr^{-1})
1408 ± 214	0-5	0.24 ± 0.02	30.5	1.79	0.37	0.34 ± 0.05	1.92 ± 0.24	5.96 ± 0.43
	5-10	0.20 ± 0.03	53.3	2.65	0.63	0.42 ± 0.03	1.32 ± 0.16	
	10-15	0.23 ± 0.04	51.7	2.28	0.64	0.53 ± 0.06	1.18 ± 0.15	
	20-25	0.23 ± 0.05	54.0	1.98	0.61	0.65 ± 0.05	1.13 ± 0.14	
	50-55	0.25 ± 0.06	33.0	2.92	0.04	0.70 ± 0.05	1.71 ± 0.21	
	70-75	0.24 ± 0.08	34.1	2.41	0.06	0.77 ± 0.06	1.72 ± 0.21	
	Mean ± 1 SD	0.23 ± 0.05	42.8 ± 11.3	2.34 ± 0.38	0.39 ± 0.26	0.57 ± 0.16	1.50 ± 0.30	

Table 3. Comparison of annual CO_2 emissions through oxidative peat decomposition (PD) with previous studies using the chamber method.

Land-use type	CO_2 emissions (gC m^{-2} yr^{-1})	Mean ground water level (m)	Treatment	Reference	Note
Oil palm plantation	1042	-0.52	Inter-rows	Dariah et al., 2014	Six years old
Oil palm plantation	930	-1.14	Inter-rows	Dariah et al., 2014	15 years old
Oil palm plantation	1800	-0.72	Inter-rows	Husnain et al., 2014	
Oil palm plantation	693	-0.58	Trenching	Melling et al., 2013	Including leaf litter decomposition
Acacia plantation	2182	-0.80	Trenching & Inter-rows	Januhiainen et al., 2012	Corrected for soil temperature
Sago plantation	762	-0.24	Trenching	Melling et al., 2013	Including leaf litter decomposition
Rubber plantation	1418	-0.67	Inter-rows	Husnain et al., 2014	
Bare ground	1718	-0.70	Inter-rows	Husnain et al., 2014	Plantations after harvesting
Mixed forest	993	-0.46	Trenching	Melling et al., 2013	Including leaf litter decomposition
Burnt forest	372	-0.14	Burning	Hirano et al., 2014	
Rubber plantation	1408	-0.69	Trenching	This study	

2.3. Discussion

2.3.1. Controls on soil CO_2 efflux

The trenching method was applied to separate oxidative peat decomposition (PD) from total soil respiration (SR). Although the trenching method has been widely applied, the method has limitations and shortcomings (Epron, 2009; Hanson et al., 2000; Subke et al., 2006) due to insufficient trenching depth, the decomposition of cut roots remaining in trenched plots, no supply of root litter through mortality and soil moisture rise caused by no transpiration. In this study, we trenched 1 m deep into peat at the middle of tree rows (Figs. 1 and 2) six months before the beginning of chamber

measurement. A study on the fine-root dynamics of rubber trees on mineral soil in northern Thailand reported that fine roots concentrated in shallow soil of 0.0–0.5 m (Maeght et al., 2015). Also, the duration, during which GWL was below 1 m, was limited except for in strong El Niño years (Fig. 4b). Thus, the trenching depth of 1 m would be sufficient in this site to avoid lateral root invasion. As for the decomposition of cut roots, during the six months after trenching including the dry season with low GWL (Fig. 4b), the majority of dead fine roots was expected to be decomposed (Comeau et al., 2016), though some, including dead coarse roots, were possibly still left and kept decomposing. The ongoing decomposition potentially led to the overestimation of PD. In contrast, the absence of live roots decreases heterotrophic respiration because of no root-litter input. However, this disturbance of no root-litter decomposition is preferable to measure PD. Although no data were available on soil moisture, if soil moisture was higher in trenched plots under low GWL conditions, microbial respiration was potentially enhanced (Ishikura et al., 2016), which could overestimate PD.

Both SR and PD were significantly depended on GWL (Figs. 7 and 8). In the wet season from December 2014 to June 2015, PD was consistently low because of high GWL near the ground surface. Such high GWL made an anoxic condition in the whole soil profile by preventing oxygen penetrating into the soil because of water saturation and consequently impeded the organic material decomposition (Hirano et al., 2009; Husen et al., 2014). In the dry season, PD increased gradually as GWL dropped deeply in unsaturated conditions and resultant high oxygen availability in the peat soil profile (Inubushi et al., 2003; Jauhiainen et al., 2005; Iiyama and Osawa, 2010). There are several studies on the relationship of soil CO_2 efflux with GWL in tropical peatland (Itoh et al., 2012; Sundari et al., 2012; Comeau et al., 2013; Hirano et al., 2014; Carlson et al., 2015; Ishikura et al., 2016). In this study, PD showed a strong negative linearity with GWL (Fig. 7), partly because GWL was lowered much by a strong El Niño drought of 2015 (Fig. 4b). Kwon et al. (2013) found that in drained peatlands, such as plantations, peat carbon was more vulnerable to drought events than in pristine peatlands. The peak of PD was measured in November, just after a lot of rain at the beginning of the wet season (Figs. 4a and 5a) probably because of stimulated microbial activity by the rain (Lee et al., 2004). In semiarid and arid ecosystems, shallowly infiltrating rainwater increased microbial respiration after a prolonged dry period (Huxman et al., 2004).

The relationship between soil CO_2 efflux and soil temperature was significant ($p < 0.05$), but with low r^2 (near = 0.15 and far = 0.14) for SR or not significant ($p > 0.05$) for PD (Fig. 6). In addition, although soil temperature was usually higher in the

afternoon, soil CO_2 efflux was not significantly different among three replications within a day ($p > 0.05$). The low temperature sensitivity of soil CO_2 efflux was attributable to the small amplitude of soil temperature both on annual (Fig. 4c) and daily bases under the tree canopy. In open peat areas, however, soil temperature positively affected soil CO_2 efflux (Schrier-Uijl et al., 2013; Jauhiainen et al., 2014). On the other hand, Hirano et al. (2014) found that the effect of soil temperature rise on soil CO_2 efflux was small even at an open peatland when GWL was low.

The residual of SR from PD, which corresponds to root respiration and leaf litter decomposition, increased in the wet season from February to June 2015 (Fig. 5c), when GWL was high near the ground surface (Fig. 4b). The seasonal variation suggests the phenology of root growth and the enhancement of litter decomposition in the wet season. The root activity of rubber trees would be positively related to the production of latex, which is higher in the wet season (Verheye, 2010). Maeght et al. (2015) found that fine roots of rubber trees began to grow three months after the beginning of the wet season, though it was a research on mineral soil. In addition, the decomposition of leaf litter was enhanced in the wet season in tropical peat swamp forests (Sundari et al., 2012). In contrast, the residual was low in the dry season. The dry soil condition probably depressed root activity. Also, rubber trees have an annual vegetative cycle with defoliation called “wintering” in the dry season (Verheye, 2010). Although the defoliation resulted in more litter accumulation in this period, litter decomposition was depressed by the desiccation condition (Hirano et al., 2009).

2.3.2. Annual CO_2 emissions

Annual soil CO_2 emissions were calculated in two manners. The significant relationships with GWL (Figs. 7 and 8) suggest that annual emissions calculated from hourly GWL are more reliable than those by averaging, though the former would be potentially underestimated to some extent because of the exclusion of pulse like CO_2 efflux due to a rain event (Lee et al., 2004). The annual PD estimated from hourly GWL (1408 ± 214 g C m^{-2} yr^{-1}) was compared with those measured at various land-use types in tropical peatlands (Table 3). Within plantations, our PD result was much lower than that of an acacia plantation with lower mean annual GWL in Sumatra, Indonesia (Jauhiainen et al., 2012). This is possibly because acacia trees could change the soil properties by increasing the level of organic carbon and total nitrogen, resulting in higher microbial biomass and basal respiration (Hergoualc'h and Verchot, 2013; Marchante et al., 2008). Our result was also lower than that of an oil palm plantation and the bare ground after deforestation (Husnain et al., 2014), but higher than those of different oil palm plantations in Sumatra (Dariah et al., 2014) and Sarawak, Malaysia

(Melling et al., 2013). On the other hand, our result was the same as PD in a rubber plantation in Sumatra (Husnain et al., 2014). To assess the annual PD, Dariah et al. (2014), Husnain et al. (2014) and Melling et al. (2013) averaged periodic flux measurements, whereas Jauhiainen et al. (2012) calculated it from monthly or quarterly GWL data using a negative linear equation. Also, Hirano et al. (2014) calculated the annual PD from half-hourly GWL data using a negative logarithmic equation determined using continuous CO_2 efflux data. In this study, PD accounted for 43% of SR (3293 g Cm^{-2} yr^{-1}) on an annual basis (Table 1). Nurzakiah et al. (2014) measured SR using a static chamber system in a nearby rubber plantation for 10 months in 2013. The mean of monthly measurements was equivalent to 723 g C m^{-2} yr^{-1}, which was much lower than our result. The low SR was due to the static chamber method with long closing time of 24 min, during which CO_2 concentration in the chamber headspace was probably almost saturated (e.g. Nakano et al., 2004). The contribution of PD was much lower than those of mature acacia (79%, Jauhiainen et al., 2012) and oil palm (71–86%, Dariah et al., 2014) plantations in Sumatra. On the other hand, the contribution of the residual (SR − PD = 1885 g C m^{-2} yr^{-1}), which corresponds to root respiration (RR) and leaf litter decomposition (LD), to SR was 57% on an annual basis (Table 1). However, the contribution of LD would have been small or negligible in plantations (Jauhiainen et al., 2012; Nagano et al., 2013). Alternatively, Hergoualc'h and verchot (2011) estimated that carbon inputs through litter fall was 150 and 510 g C m^{-2} yr^{-1} in oil palm and acacia plantations, respectively. Assuming that the litter fall at the rubber plantation was equivalent to the average (330 g C m^{-2} yr^{-1}) of the two values and the litter fall was all decomposed in a year, annual RR is calculated to be 1555 g Cm^{-2} yr^{-1} or 47% of SR. This RR contribution was much higher than those of acacia (21%, Jauhiainen et al., 2012) and oil palm plantations in Sumatra (17–29%, Dariah et al., 2014), but lower than a mixed swamp forest (60%), oil palm plantation (62%) and sago plantation (52%) in Sarawak (Melling et al., 2013).

SR was measured at near and far positions from rubber trees to examine the spatial distribution of RR. It is reported that SR depends on distances from trees and is expected to be free of RR contribution at far positions in acacia and oil palm plantations (Jauhiainen et al., 2012; Dariah et al., 2014). Unexpectedly, however, no significant difference was found in SR between at near and far positions from rubber trees ($p > 0.05$) (Table 1). This result indicates that RR did not decrease with a distance from trees up to 3 m, around the middle of tree rows. Roots of rubber trees could explore and intermingle in the inter-space of tree rows by seven years after planting (Pathiratna, 2006). Moreover, the compacted peat condition in this site probably

enhanced root development (Melling et al., 2013). A large standard deviation (SD) in SR in comparison with PD (Table 1) suggests a large spatial variation in RR.

This study was conducted in a strong El Niño year of 2015, in which the dry season was prolonged, and GWL lowered more. Thus, PD was expected to be larger than in normal years without El Niño drought. To assess the effect of the El Niño drought in 2015, PD was calculated from GWL data during the dry seasons (June to November) in 2014 and 2015 using the linear relationships (Fig. 7). Mean seasonal GWL was lower by 0.35 m in 2015 than in 2014, a weak El Niño year. Seasonal PD was 675 and 1139 g C m^{-2}, respectively, for 2014 and 2015; the latter was about 70% higher than the former.

2.3.3. Contribution of peat decomposition to total subsidence

After correction for GWL variation, annual subsidence rates of 5.64 ± 3.20 and 5.96 ± 0.43 cm yr^{-1} were found from outside and inside of trenching, respectively, during an El Niño year from December 2014 to December 2015. The rubber plantation had been drained for more than eight years, and the mean annual GWL was −0.69 m. Because ground elevation was sensitive to GWL (Fig. 9), elevation should be measured at short intervals simultaneously with GWL monitoring to determine annual subsidence correctly. The annual subsidence was higher than those measured at other plantations on tropical peat. For example, annual subsidence rates at acacia and oil palm plantations in Sumatra with mean annual GWL of −0.70 m were 4.2 and 5 cm yr^{-1}, respectively, more than five years after initial drainage began (Couwenberg and Hooijer, 2013; Hooijer et al., 2012). Using field data for over 20 years, Nagano et al. (2013) reported that annual subsidence was in the range of 3.1–5.2 cm yr^{-1} in degraded peatland with mean GWL of −0.6 m. In addition, mean annual subsidence rates of 2 and 3 cm yr^{-1} were reported for a drained peatland and an agricultural field in Malaysia, respectively (Wosten, 1997; Murayama and Bakar, 1996a). The larger subsidence in this study is attributable to low GWL caused by the strong El Niño drought.

Annual subsidence resulting from oxidative peat decomposition (1408 g C m^{-2} yr^{-1}) was simply calculated to be 1.50 cm yr^{-1}, which accounted for 25% of total subsidence of 5.96 cm yr^{-1} in the trenching (Table 2). The contribution of 25% was much lower than 60, 50–70, 92 and 40–60%, respectively, from a degraded peatland (Wosten, 1997), an agricultural field (Murayama and Bakar, 1996b), oil palm and acacia plantations, (Hooijer et al., 2012) and a meta-analysis (Couwenberg et al., 2009). Hooijer et al. (2012) calculated PD subsidence using the contribution of 92% to be 2129 and 1856 g C m^{-2} yr^{-1}, respectively, for oil palm and acacia plantations in Sumatra. On the other hand, the annual subsidence of 1.50 cm yr^{-1} due to peat

oxidation in this study was similar to those (1.53 ± 0.70 cm yr^{-1}) of degraded peat swamp forests in Central Kalimantan, though annual PD was estimated to be low at 790 g C m^{-2} yr^{-1} (Hooijer et al., 2014). Crucial parameters to interconvert subsidence and oxidative peat decomposition are peat properties, such as BD and carbon content (Könönen et al., 2015). Higher subsidence rates usually result from low values of BD and carbon content (Murayama and Bakar, 1996a) (Eq. (2)). In other words, low BD and carbon content result in low PD for the same subsidence. In this study, BD was over 0.20 g cm^{-3} at all depths (Table 2) probably because of compaction during land preparation. The BD was much higher than those of oil palm and acacia plantations in Sumatra (0.075–0.15 g cm^{-3}) (Hooijer et al., 2012) and undisturbed peatlands in Central Kalimantan (0.098 g cm^{-3}) (Shimada et al., 2001). In addition, carbon content of 42.8% in this study (Table 2) was lower than an average of 55% (Hooijer et al., 2012; Shimada et al., 2001). The lower carbon content, especially in the surface soil (0–5 cm), was possibly due to the flooding of Kahayan river running about 1 km distant from the study site. As a result, peat carbon density, as a product of BD and carbon content, of 0.086 g C cm^{-3} in this study was higher than 0.054 (Shimada et al., 2001) and 0.041–0.083 g C cm^{-3} (Hooijer et al., 2012). The lower contribution (25%) of PD to total subsidence was attributable to the higher carbon density due to compaction.

This chapter was published as
Wakhid, N., Hirano, T., Okimoto, Y., Nurzakiah, S., Nursyamsi, D., 2017. Soil carbon dioxide emissions from a rubber plantation on tropical peat. Sci. Total Environ. 581–582: 857–865. http://dx.doi.org/10.1016/j.scitotenv.2017.01.035.

Chapter 3. Net primary production and CO_2 emission through frond decomposition in oil palm plantations on peat in Sumatra

3.1. Material and methods

3.1.1. Study site

The study was conducted from February 2018 to July 2019 in two oil palm (*Elaeis guineensis*) plantations on peat soil in Sumatra, Indonesia. The first oil palm plantation site was an industrial plantation on peat soil in Riau, Sumatra, Indonesia (0° 42' 16" N, 101° 42' 52.8" E). Annual precipitation in 2018 was 2046 mm yr^{-1} in the plantation, almost identical to the mean between 2011 and 2018 (2033 ± 339 mm yr^{-1}, mean ± 1 standard deviation (SD)). Monthly precipitation was less than 100 mm in January, May, and July. The annual mean air temperature was 27.5°C at a meteorological station 50 km away (BPS-Statistics of Riau province, 2019). The palm tree cultivar was Marihat (M) with a tree density of 148 trees ha^{-1}. In 2019, the tree age was 15 years. The peat depth was 0.8 m in average. Annual mean groundwater level (GWL) was -0.5 m, varying seasonally between -0.2 and -0.8 m. GWL was high from November to January and low from May to August. The ground surface except in a circle with a radius of 2 m from a tree base and in harvesting path was densely covered with fern plants (*Nephrolepis biserrata*). The other understory vegetation was *Axonopus compressus*, *Asystasia micrantha*, *Peperomia pellucida*, and *Asplenium longissimum*. Fertilizers were applied twice a year that equivalent to 139 kg N, 55.5 kg P_2O_5, 222 kg K_2O, 500 kg $CaCO_3$, 278 kg CaO and 2.96 kg CuZn (ha^{-1} yr^{-1}).

The second oil palm plantation was a smallholder plantation on peat soil in Jambi, Sumatra, Indonesia (1° 14' 20" S, 103° 35' 23" E). Annual precipitation in 2018 was 1952 mm yr^{-1} at a meteorological station 28 km away, similar to the mean between 2013 and 2018 (2065 ± 401 mm yr^{-1}, BPS-Statistics of Tanjung Jabung Timur Regency, 2019). Monthly precipitation was less than 100 mm in June and July. Annual mean air temperature was 27.9°C at a meteorological station 25 km away (BPS-Statistics of Tanjung Jabung Timur Regency, 2019). The tree density was 125 trees ha^{-1} with two cultivars in the same field, Marihat (*M*) and Sofin (*S*), with the ratio of 4:1 (*M* : *S*). Oil palm trees were planted in 1994 or about 25 years old in 2019. Annual mean GWL was -0.2 m, that varying seasonally between 0.1 and -0.8 m. Annual GWL was high from March to May and low from June to September. The ground surface except in a circle with a radius of 2 m from every tree base was sparsely covered with *Axonopus compressus*. The other understory vegetation was similar to those in Riau above. Fertilizer was applied twice a year on average of 64.8 kg N, 64.8 kg P_2O_5, 64.8

kg K_2O and 2 kg MgO (ha^{-1} yr^{-1}). However, fertilization was not regular, depending on the farmer's finance condition. Both plantations are mature in a common 25-year cycle of renovation (Corley and Tinker, 2003).

3.1.2. Above- and belowground net primary production

Net primary production (NPP, Mg C ha^{-1} yr^{-1}) was calculated as all plant biomass produced during a specified period. Aboveground NPP (ANPP) was estimated as the sum of tree canopy (trunks and attached fronds), pruned frond, fruit bunch, and understory vegetation production. Tree canopy NPP was calculated as a cumulative biomass increment (mass difference) between February 2018 and January 2019 for Riau, and between March 2018 and February 2019 for Jambi using the following allometric equation for mature trees (Khasanah et al., 2015):

$$\text{Canopy biomass (Mg tree}^{-1}) = 0.0939 \times H + 0.0951 \quad (3)$$

where H (m) is the length from the ground level to the base of frond number 41, which is the lowest frond maintained in the canopy under normal management (Khasanah et al., 2015). H was measured in February 2018 and January 2019 in Riau, and in March 2018 and February 2019 in Jambi, for 32 and 25 trees, respectively, in Riau and Jambi, which correspond to about 20% of tree density. In Jambi, two cultivars of Marihat (*M*) and Sofin (*S*) were planted, and the ratio of these cultivars was roughly estimated to be 4:1 in tree density. Thus, the numbers of sample trees were 20 for *M* and 5 for *S*. In addition, to calculate NPP, weighting factors of 0.8 and 0.2 were applied for the two cultivars, respectively.

Annual fruit bunch NPP was estimated from yield data recorded by the company in Riau and the farmer in Jambi, respectively. As there is no data about yield difference between *M* and *S* in Jambi, fruit bunch production of the two cultivars was assumed to be the same. Dry weight and carbon (C) content of fruit bunches were determined using three fresh fruit bunches of *M* in Riau. A frond attached just under a fruit bunch is pruned when the fruit bunch is harvested, and the pruned frond is left on the ground to return the nutrients from the frond to the soil. On average, one frond was pruned monthly from one tree both in Riau and Jambi. Dry weight and C content were measured for five pruned fronds of each cultivar in Riau and Jambi. Understory vegetation biomass was measured by destructive sampling from three quadrats of 0.5 m × 0.5 m in three management areas (nine quadrats in each site): (1) root circles (RC) with a radius of 1 m oil palm tree bases, (2) inter-rows between frond stacks (FS), where pruned fronds were piled up, and (3) harvesting paths (HP). Understory

vegetation was harvested in September 2018, February 2019 and June 2019 in Riau and in September 2018, March 2019 and July 2019 in Jambi. Then annual NPP of understory vegetation was calculated as a difference between maximum and minimum biomass of each sampling (Scurlock et al., 2002).

Belowground NPP (BNPP) was calculated from the production of coarse and fine roots biomass. Coarse root biomass was calculated using the following empirical equation (Syahrinudin, 2005):

$$\text{Coarse root biomass (including trunk bases, Mg ha}^{-1}) = 1.45 \times \text{palm age} + 9.88 \quad (4)$$

This equation was developed for an oil palm plantation on mineral soil with tree density of 140 trees ha^{-1}. Thus, to adjust the tree densities of our sites (148 and 125 trees ha^{-1}), calculated biomass was corrected with factors of 1.06 (148/140) and 0.89 (125/140) for Riau and Jambi, respectively. Annual coarse root NPP was calculated as an annual biomass increase. C content of fine root was used for coarse root NPP calculation.

Fine root NPP (≤ 2 mm in diameter) was estimated by sequential soil coring for a depth of 0-30 cm using an auger with a diameter of 2.54 cm. Core sampling was conducted in February 2018, September 2018, and February 2019 in Riau and in March 2018, September 2018, and March 2019 in Jambi around three trees at different distances from a ditch (only around one tree in February 2018 in Riau). In Jambi, one tree and two trees were selected from cultivars *S* and *M*, respectively. For each tree, soil cores were collected at 1, 2, and 3 m distance from the base in four directions (Fig. 10). The sampling layout included root circles, understory vegetation areas, frond stacks, and harvesting paths. Totally, 12 soil core samples around each tree were collected. Soil cores were stored in plastic bags and washed with tap water to separate roots from peat soil. By sieving, only fine roots of oil palm trees were extracted and then separated into living (biomass) and dead ones (necromass) by visual inspection based on color and shape (Makkonen and Helmisaari, 1999). Fine roots of oil palm trees were rough, rigid and a little bit dark in color, whereas roots of understory vegetation were distinguished by their light color, and soft without a lignified periderm (Leuschner et al., 2009). Fine root production, mortality, and decomposition between sampling dates were estimated by a simplified decision matrix method (Yuan and Chen, 2013), and annual fine root NPP was calculated as the sum of production. In Jambi, fine root NPP was determined as the sum of those of *M* and *S* cultivars, considering their shares in tree density (80% vs. 20%).

To measure the dry weight of frond (leaves and rachises), fruit bunch, fine root,

and understory vegetation, samples were dried at 70°C for at least 48 hours. C concentration of those components was determined by the loss of ignition (LoI) method at 550°C in a muffle furnace (Thermolyne type 48000, USA) with a conversion factor of 0.58 from organic matter to organic C. Nitrogen (N) content of pruned fronds was determined with the Kjeldahl technique.

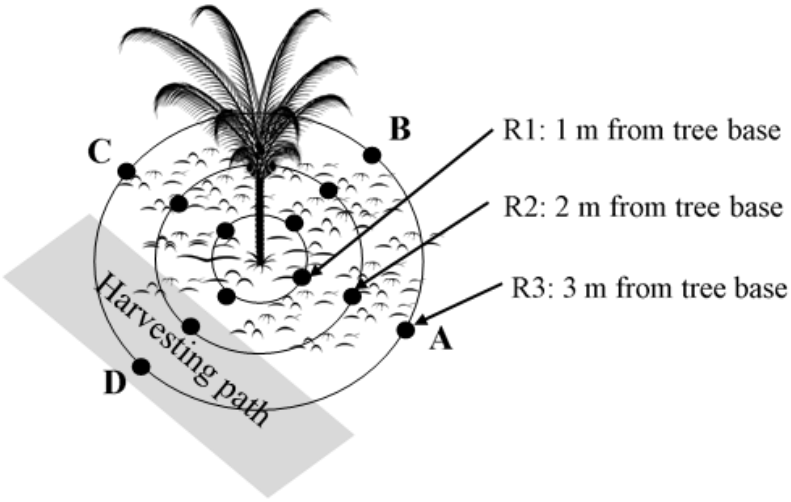

Fig. 10. Scheme of sequential soil core sampling at different distances and areas from oil palm tree base.

3.1.3. Litter/ frond decomposition

Frond decomposition was measured using litter bags of 40 cm x 80 cm, which were made of plastic mosquito netting with a mesh size of 2 mm (Fig. 11). Fronds immediately after cutting down were collected and separated into two parts (tip and base) because of their large size. Tips and bases were put into bags separately. In Riau, 100 bags were prepared for each of tips and bases and set on the top of frond heaps in February 2018. However, in total, only 99 bags were retrieved in September 2018, January 2019, and June 2019 as most of litter bags were missing. In Jambi, 18 bags were prepared for each of tips and bases of the two cultivars (*M* and *S*), respectively. 36 bags in total were set equally on the top of and under frond heaps, respectively, in February 2018. Three bags of each condition were retrieved from the two positions in September 2018, February 2019 and July 2019, respectively. After retrieved, each of litterbags was carefully cleaned to remove external materials such as soil and litter particles. Dry weight was measured by drying samples at 70°C for at least 48 hours, and C content was determined by the loss of ignition (LoI) method at 550°C in a muffle furnace (Thermolyne type 48000, USA) with a conversion factor of 0.58 from organic matter to organic C (Agus et al., 2011). Also, initial values of dry weight and C content

of leaves and rachis were measured at the beginning (n = 3). The residual ratio of dry weight or C amount was plotted against elapsed time, and a simple negative exponential equation was fitted to determine the decomposition rate constant (k). Using the k value and initial C amount, C loss through the decomposition of pruned fronds was estimated. Moreover, under the assumption that C loss was caused by only oxidative decomposition, area-based CO_2 emission was calculated monthly and summed up annually using pruned frond production.

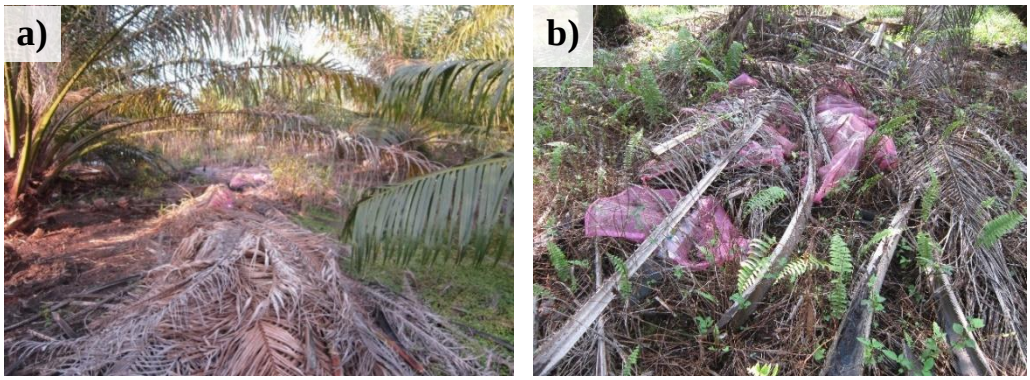

Fig. 11. Frond in the oil palm plantations (a) pruned fronds were piled up in the frond stack, (b) litter bags for frond decomposition measurement were set up together with the pruned fronds in the frond stack.

3.1.4. Data analysis

Data were compared among/ between sites, cultivars, components and locations by ANOVA and Tukey's HSD test using R software (R Development Core Team 2019; version 3.5.3).

3.2. Results

3.2.1. Characteristic of oil palm component

C content of pruned frond in Riau and Jambi was in the range of 53-57% (Table 4). C and N contents were not significantly different between tip and base parts, but significantly different between leaf and rachis. CN ratio was significantly higher in rachis than in leaf. *S* in Jambi has the lowest CN ratio than *M* in Riau and Jambi, respectively. C content of the components of oil palm plantations ranged between 52 and 58%, which was highest in fruit bunches, followed by fine roots, fronds and understory vegetation (Table 5).

3.2.2. Aboveground and belowground net primary production (ANPP and BNPP)

M in Riau had the highest height increment, followed by *S* and *M* in Jambi (Table 6). As a result, biomass growth of *M* in Riau was higher than *S* and *M* in Jambi. Area-based biomass growth of *M* was higher than that of *S* because of different tree density in Jambi. Understory vegetation biomass in frond stacks was significantly larger than those in root circles and harvesting paths in Riau (Table 7). In contrast, no significant difference was found in Jambi. Understory vegetation biomass showed significant seasonal difference in both sites, but the pattern was different. In August 2018, biomass was largest in Riau but smallest in Jambi, which was reversed in July 2019.

Fine root biomass decreased with distance from tree bases both in Riau and Jambi (Table 8). Fine root biomass also showed significant seasonality. In Riau, fine root biomass in February 2019 (wet season) was significantly higher than in September 2018 (dry season). In Jambi (*M* and *S*), fine root biomass showed no significant difference between February 2019 and September 2018, but in February 2019 it was significantly higher than in February 2018. In contrast to biomass, fine root necromass in Riau showed no significant difference between positions and seasons. However, necromass of *M* and *S* in Jambi were significantly different between positions from tree bases. Fine root biomass of *S* was significantly higher than that of *M* in Jambi. However, fine root necromass of *M* in Riau was significantly lower than that of *M* in Jambi. Fine root production (NPP) showed no seasonal variation between two periods of sampling in Riau (Table 9). However, in Jambi, fine root productions of *M* and *S* were significantly different between two periods. There was no seasonal variation of fine root mortality in both sites. For fine root decomposition, only *M* in Jambi showed a significant seasonal difference between the two periods. Fine root production, mortality and decomposition were not significantly different between cultivars (*M* vs. *S* in Jambi) and between sites (*M* in Riau vs. *M* in Jambi).

Annual total NPP was estimated to be 17.3 and 13.5 Mg C ha^{-1} yr^{-1} in Riau and Jambi, respectively (Table 10). The total NPP in Riau was higher than that in Jambi. ANPP was higher in Riau, but BNPP was higher in Jambi. Total NPP was dominated by ANPP (14.0 (Riau) and 9.9 (Jambi) Mg C ha^{-1} yr^{-1}), which accounted for 81 and 73% in Riau and Jambi, respectively. Fruit bunch production contributed most to NPP, accounted for 35 and 34% in Riau and Jambi, respectively. Annual BNPP was 3.32 and 3.60 Mg C ha^{-1} yr^{-1}, respectively, in Riau and Jambi, of which fine root production accounted for 74 and 80 % in Riau and Jambi, respectively (Table 10).

3.2.3. CO_2 emission through pruned frond decomposition

The dry weight of a whole pruned frond was 2578, 2254, 3387 g frond^{-1} for *M* in Riau, and *M* and *S* in Jambi, respectively (Table 4). The frond of *S* was 1.3-1.5 times larger than that of *M* in Jambi. C amount of pruned fronds from three cultivars averaged at 1432 ± 289, 1259 ± 104, and 1872 ± 314 g C frond^{-1} (mean ± 1 SD, n = 5)) for *M* in Riau, and *M* and *S* in Jambi, respectively.

The temporal pattern of C loss through pruned frond decomposition was following a negative exponential (Fig. 12). In Riau, the number of litter bags in the second and third retrieving was different from the first retrieving because some of bags were lost during the study (n = 45, 27, and 27 litter bags, for the first, second, and third retrieving, respectively). Therefore, without distinguishing tip and base parts, all retrieved samples were plotted for decomposition rate calculations. As a result, the frond decomposition rate constant (k) in Riau was estimated to be 1.86 yr^{-1}. Using the k, the pruned frond of *M* in Riau was estimated to be decomposed by 90% in 1.25 years. Annual carbon input through pruned fronds into the plantation was estimated to be 2.54 Mg C ha^{-1} yr^{-1} (= annual pruned fronds (12 fronds tree^{-1}) × dry weight (2578 g frond^{-1}) × C content (55.5 %) × tree density (148 trees ha^{-1})), whereas annual CO_2 emission through oxidative frond decomposition in Riau was calculated to be 1.48 Mg C ha^{-1} yr^{-1}.

In Jambi, the k values were not significantly different among tip and base parts, top and below heap of pruned fronds, and among two cultivars, *M* and *S*. However, total CO_2 emissions through frond decomposition should be different between the cultivars because of the different frond size. Thus, using all data for each cultivar (n = 12 for each retrieving, respectively, for *M* and *S*), k values were determined to be 1.57 and 1.81 yr^{-1} for *M* and *S*, respectively (Fig. 12). From those k values, the pruned fronds of *M* and *S* in Jambi were estimated to be decomposed by 90% in 1.50 and 1.25 years, respectively. Annual carbon input through pruned frond into the plantation in Jambi for each cultivar was 1.51 and 0.56 Mg C ha^{-1} yr^{-1}, respectively, for *M* and *S*. Annual CO_2 emission through frond decomposition was estimated to be 0.80 and 0.32 Mg C ha^{-1} yr^{-1}, respectively, for *M* and *S* in Jambi. In total, annual carbon input and CO_2 emissions from pruned frond in Jambi were estimated to be 2.07 and 1.12 Mg C ha^{-1} yr^{-1}, respectively.

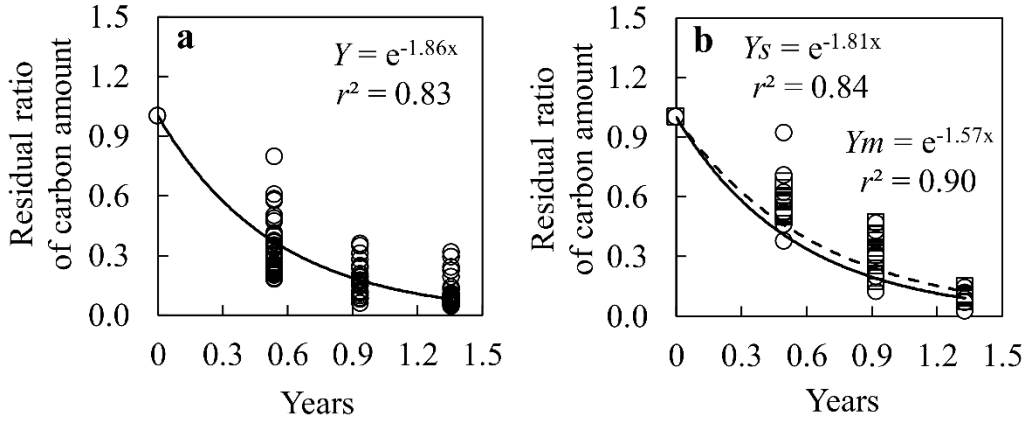

Fig. 12. C loss pattern of a) *M* in Riau and b) *M* (squares, dash line) and *S* (circles, solid line) in Jambi. y_m and y_s represent the fitted equations for *M* and *S* in Jambi, respectively.

Table 4. Initial amount of carbon (C), nitrogen (N), CN ratio, and water content (WC) of frond in Riau and Jambi (mean ± 1 SD, *n* = 3).

Samples	C (%)	N (%)	CN ratio	WC (%)
Marihat (*M*) in Riau				
(dry weight = 2578 ± 509 g frond^{-1}, *n* = 5)				
Leaf (tip)	54.6 ± 0.54	1.23 ± 0.58	50.3 ± 19.1	59.3 ± 0.3
Rachis (tip)	56.7 ± 0.28	0.38 ± 0.13	160.9 ± 58.9	60.2 ± 8.3
Leaf (base)	55.0 ± 0.29	1.62 ± 0.44	35.4 ± 8.4	59.1 ± 1.6
Rachis (base)	55.6 ± 0.35	0.39 ± 0.06	143.7 ± 20.0	37.8 ± 6.6
Marihat (*M*) in Jambi				
(dry weight = 2254 ± 188 g frond^{-1}, *n* = 5)				
Leaf (tip)	54.0 ± 0.33	1.90 ± 0.33	29.2 ± 5.7	54.9 ± 2.7
Rachis (tip)	57.1 ± 0.07	0.66± 0.08	87.2 ± 11.4	65.9 ± 4.2
Leaf (base)	54.4 ± 0.40	2.00 ± 0.19	27.4 ± 2.3	58.5 ± 2.3
Rachis (base)	56.9 ± 0.25	0.60 ± 0.10	96.2 ± 15.4	71.1 ± 7.5
Sofin (*S*) in Jambi				
(dry weight = 3387 ± 567 g frond^{-1}, *n* = 5)				
Leaf (tip)	53.1 ± 0.89	2.27 ± 0.16	23.5 ± 1.5	50.1 ± 11.4
Rachis (tip)	56.8 ± 0.09	0.75 ± 0.13	77.0 ± 13.3	69.8 ± 3.7
Leaf (base)	53.6 ± 1.32	2.15 ± 0.51	25.9 ± 6.0	56.5 ± 2.6
Rachis (base)	56.4 ± 0.11	0.79 ± 0.20	74.9 ± 20.6	71.1 ± 4.8
ANOVA (*P* value)				
Component (leaf vs. rachis)	<0.001	<0.001	<0.001	0.21
Position (tip vs. base)	0.76	0.64	0.68	0.50
Site (*M* in Riau vs. *M* in Jambi)	0.74	0.18	0.08	0.13
Cultivar (*M* vs. *S* in Jambi)	0.42	0.06	<0.05	0.16
Interaction (component-position)	<0.05	0.62	0.98	0.06

Table 5. C content (%) of each component of oil palm plantation (mean ± 1 SD). Different alphabets in Riau denote significant difference ($P < 0.05$) according to Tukey HSD test after ANOVA.

Component	Riau	Jambi	
		M	*S*
Frond (leaf and rachis)	55.5 ± 0. 9a (*n* =12)	55.6 ± 1.5 (*n* = 12)	55.0 ± 1.9 (*n* = 12)
Fruit bunch	57.7 ± 0.06a (*n* = 3)	n/a	
Understory vegetation	51.9 ± 3.2b (*n* = 9)	53.5 ± 1.8 (*n* = 9)	
Fine root	56.7 ± 1.1a (*n* = 6)	n/a	
ANOVA (*P* value)	<0.001		

Table 6. Tree height and canopy biomass (mean ± 1 SD; *n* = 32, 20 and 5 for *M* in Riau, *M* in Jambi, and *S* in Jambi, respectively).

Component		Riau	Jambi	
		M	*M*	*S*
Tree height (m)	Feb./ Mar. 2018	3.78 ± 1.37	4.03 ± 1.27	4.02 ± 0.65
	Feb./ Mar. 2019	4.35 ± 1.24	4.38 ± 1.31	4.44 ± 0.71
Height growth (m yr^{-1})		0.57 ± 0.88	0.35 ± 0.24	0.42 ± 0.32
Biomass (Mg $tree^{-1}$)	Feb./ Mar. 2018	0.45 ± 0.13	0.47 ± 0.12	0.47 ± 0.06
	Feb./ Mar. 2019	0.50 ± 0.12	0.51 ± 0.12	0.51 ± 0.07
Biomass growth (Mg $tree^{-1}$ yr^{-1})		0.05 ± 0.08	0.03 ± 0.02	0.04 ± 0.03
Tree density (trees ha^{-1})		148	100	25
Biomass (Mg ha^{-1})	Feb./ Mar. 2018	66.6	47.3	11.8
	Feb./ Mar. 2019	74.5	50.6	12.8
Biomass growth (Mg ha^{-1} yr^{-1})		7.9	3.3	1.0

Table 7. Understory vegetation biomass **(**mean ± 1 SD, n = 3). Different alphabets in the column for Riau (*) and in seasonal means for Riau and Jambi, respectively, denote significant difference ($P < 0.05$) according to Tukey HSD test after ANOVA.

Area	Biomass (Mg ha^{-1})							
	Aug. 2018		Jan. 2019		Jul. 2019		Mean	
	Riau	Jambi	Riau	Jambi	Riau	Jambi	Riau*	Jambi
Root circle	1.12 ± 0.88	0.52 ± 0.41	0.62 ± 0.73	1.87 ± 0.65	0.04 ± 0.04	1.43 ± 1.88	0.59 ± 0.54b	1.27 ± 0.69
Harvesting path	0.62 ± 1.00	1.00 ± 0.17	0.39 ± 0.09	1.94 ± 0.99	0.19 ± 0.07	4.16 ± 2.21	0.40 ± 0.22b	2.37 ± 1.62
Frond stack	7.76 ± 1.31	1.14 ± 0.71	4.78 ± 1.07	2.52 ± 0.84	4.77 ± 0.99	1.86 ± 1.28	5.77 ± 1.72a	1.84 ± 0.69
Mean	3.17 ± 3.98a	0.89 ± 0.32(b)	1.93 ± 2.47b	2.11 ± 0.36(ab)	1.67 ± 2.69b	2.48 ± 1.46(a)	2.25 ± 3.05	1.83 ± 0.55

ANOVA (P value)	Riau	Jambi
Area	<0.001	0.18
Season	<0.01	<0.05
Interaction (area-season)	<0.05	0.23
Site	0.48	

Table 8. Biomass and necromass (Mg ha^{-1}) of fine roots (mean ± 1 SD; n = 4 for Feb. 2018 in Riau, 12 for Sep. 2018 and Feb. 2019 in Riau, 8 for *M* in Jambi, and 4 for *S* in Jambi). Different alphabets in seasonal mean values in biomass (*) denote significant difference at positions ($P < 0.05$) and in positional mean values denote significant difference in seasonal variations ($P < 0.05$), for each of Riau, Jambi *M* and Jambi *S*, respectively, according to Tukey HSD test ($P < 0.05$) after ANOVA.

Site and position	Feb. 2018		Sep. 2018		Feb. 2019		Mean	
	Biomass	Necromass	Biomass	Necromass	Biomass	Necromass	Biomass*	Necromass
Riau								
1m	1.90 ± 1.44	0.48 ± 0.30	1.46 ± 1.09	1.17 ± 2.77	4.98 ± 4.37	2.04 ± 1.28	2.78 ± 1.92a	1.23 ± 0.78
2m	2.98 ± 1.63	0.59 ± 0.19	0.77 ± 0.64	1.04 ± 3.20	2.36 ± 1.35	0.56 ± 0.44	2.04 ± 1.14ab	0.73 ± 0.27
3m	1.52 ± 0.68	0.43 ± 0.47	0.75 ± 1.04	0.00 ± 0.00	2.17 ± 1.70	0.58 ± 0.60	1.48 ± 0.71b	0.34 ± 0.30
Mean	2.13 ± 0.08ab	0.5 ± 0.08	0.99 ± 0.4b	0.74 ± 0.64	3.17 ± 1.57a	1.06 ± 0.85	2.10 ± 0.65	0.77 ± 0.45
Jambi *M*								
1m	1.04 ± 0.95	1.11 ± 0.85	4.87 ± 1.34	2.58 ± 1.58	6.05 ± 3.60	2.55 ± 1.06	3.98 ± 2.62a	2.08 ± 0.84
2m	0.16 ±0.15	0.24 ± 0.21	1.79 ± 1.52	1.35 ± 0.73	2.87 ± 1.93	1.86 ± 1.35	1.61 ± 1.36b	1.15 ± 0.83
3m	0.35 ± 0.70	0.48 ± 0.41	1.38 ± 1.27	0.74 ± 0.63	1.82 ± 1.45	0.86 ± 0.77	1.18 ± 0.75b	0.69 ± 0.19
Mean	0.52 ± 0.40b	0.61 ± 0.45(a)	2.68 ± 1.91a	1.56 ± 0.94(b)	3.58 ± 2.20a	1.76 ± 0.85(b)	2.26 ± 1.51	1.31 ± 0.71
Jambi *S*								
1m	1.59 ± 1.17	1.87 ± 0.75	8.67 ± 3.91	3.06 ± 0.94	9.08 ± 2.47	2.52 ± 1.11	6.45 ± 4.21a	2.48 ± 0.59
2m	1.75 ± 0.62	1.21 ± 0.28	3.02 ± 0.56	1.22 ± 1.24	3.14 ± 0.74	1.88 ± 0.98	2.64 ± 0.77b	1.44 ± 0.39
3m	0.70 ± 0.47	1.15 ± 0.45	3.58 ± 2.27	0.84 ± 0.63	2.00 ± 1.37	1.40 ± 1.35	2.09 ±1.44b	1.13 ± 0.28
Mean	1.35 ± 0.56b	1.41 ± 0.40	5.09 ± 3.11a	1.70 ± 1.19	4.74 ± 3.80a	1.94 ± 0.56	3.73 ± 2.37	1.68 ± 0.71

ANOVA (P value)	Biomass in Riau	Necromass in Riau	Biomass *M* in Jambi	Necromass *M* in Jambi	Biomass *S* in Jambi	Necromass *S* in Jambi
Position	<0.05	0.06	<0.001	<0.001	<0.001	<0.01
Season	<0.001	0.31	<0.001	<0.001	<0.001	0.38
Interaction position-season	<0.05	0.26	<0.01	0.24	<0.01	0.48
	0.71	<0.05				

Site (*M* in Riau vs. *M* in Jambi)		
Cultivar (*M* vs. *S* in Jambi)	<0.05	0.11
Interaction cultivar-season	0.44	

Table 9. Fine root production (NPP), mortality, and decomposition in Riau and Jambi (mean ± 1 SD; n = 12 for Feb. to Sept. 2018 in Riau, 36 for Sep. 2018 to Feb. 2019 in Riau, 24 for *M* in Jambi, and 12 for *S* in Jambi). Lower case letters indicate significant difference in seasonal productions according to Tukey HSD test ($P < 0.05$) after ANOVA.

Site	February to September 2018			September 2018 to February 2019			Annual		
	Mg C ha^{-1} $period^{-1}$						(Mg C ha^{-1} yr^{-1})		
	Production (NPP)	Mortality	Decomposition	Production (NPP)	Mortality	Decomposition	Production (NPP)	Mortality	Decomposition
Riau	0.65 ± 1.91	1.12 ± 1.51	0.83 ± 0.91	1.80 ± 2.09	0.56 ± 0.66	0.38 ± 1.50	2.45 ± 2.86	1.69 ± 1.64	1.22 ± 1.67
Jambi *M*	1.83 ± 1.56a	0.60 ± 0.74	0.06 ± 0.14	0.97 ± 1.32b	0.47 ± 0.59	0.35 ± 0.60	2.80 ± 2.33	1.07 ± 0.92	0.41 ± 0.57
Jambi *S*	2.48 ± 2.26a	0.36 ± 0.52	0.19 ± 0.22	0.62 ± 1.26b	0.82 ± 0.79	0.69 ± 0.94	3.10 ± 2.49	1.18 ± 0.81	0.88 ± 0.85
ANOVA (P value)	Prod. in Riau	Mortal. in Riau	Decomp.in Riau	Prod. *M* in Jambi	Mortal. *M* in Jambi	Decomp. *M* in Jambi	Prod. *S* in Jambi	Mortal.*S* in Jambi	Decomp. *S* in Jambi
Season	0.10	0.08	0.33	<0.05	0.49	<0.05	<0.05	0.11	0.09
	Production (NPP)	Mortality	Decomposition						
Cultivar (*M* and *S* in Jambi)	0.72	0.74	0.09						
Interaction cultivar-season	0.20	0.08	0.40						
Site (*M* in Riau vs. *M* in Jambi)	0.76	0.31	0.17						

Table 10. Net primary production (NPP) based on biomass and carbon.

Component	NPP based on Biomass (Mg ha^{-1} yr^{-1})		NPP based on Carbon (Mg C $ha^{-1}yr^{-1}$)	
	Riau	Jambi	Riau	Jambi
Aboveground NPP (ANPP)				
Tree canopy	7.92	4.25	4.45	2.42
Pruned frond	4.58	3.72	2.54	2.07
Fruit bunch	10.6	7.85	6.13	4.53
Understory vegetation	1.50	1.60	0.85	0.88
Total	24.6	17.4	14.0	9.9
Belowground NPP (BNPP)				
Coarse root	1.53	1.29	0.87	0.73
Fine root	4.32	5.04	2.45	2.86
Total	5.85	6.34	3.32	3.60
Total NPP (ANPP + BNPP)	30.5	23.8	17.3	13.5

3.3. Discussion

3.3.1. ANPP (including understory)

The ANPP was higher in Riau than in Jambi. Within four components of ANPP, the largest one was fruit NPP, which was higher in Riau than in Jambi (Table 10). Age difference was attributable to this difference. Oil palm production usually peaks between 8 and 16 years old and declines after 24 years old (Corley and Tinker, 2003). Furthermore, the plantation in Riau was an industrial plantation. Palm tree management, such as cultivar quality, fertilizer application, and pest control, was expected to be better in Riau. According to the data from Directorate general of estate crops, Indonesia Ministry of Agriculture (2017), the fruit yield productivity of industrial plantations was higher than that of smallholder plantations. Our results of 6.13 and 4.53 Mg C ha^{-1} yr^{-1}, respectively, in Riau and Jambi were almost consistent with the productivity data of industrial plantations in Riau (7.1 Mg C ha^{-1} yr^{-1}) and smallholder plantations in Jambi (4.6 Mg C ha^{-1} yr^{-1}), which are converted from 4.91 and 3.19 Mg ha^{-1} yr^{-1} of crude palm oil (CPO) production data in industrial plantations in Riau and smallholder plantations in Jambi, respectively (Directorate general of estate crops, Indonesia Ministry of Agriculture, 2017); CPO was assumed to be 20 % of fresh fruit bunches (FFB) with dry weight (50%) and C content (57.7%). The lower tree canopy, fresh fruit bunches, and pruned frond NPP in Jambi (Table 10) were also related to the tree age. Palm tree growth decreased after 21 years old (Henson, 2017). Moreover, frond growth of oil palm tends to decline along with aging (Syahrinudin,

2005). Also, pruned frond NPP was partly influenced by the cultivar type that results in different frond size, which was found between the two cultivars in Jambi.

Understory vegetation NPP showed a similar result in Riau and Jambi (Table 7). In Riau, understory vegetation biomass in frond stacks was higher than in other areas, whereas in Jambi, the result was not significantly different among three areas. The larger biomass in frond stacks in Riau (about 2 m around the tree base) was due to the dense cover of fern plants (*Nephrolepis biserrata*) which was kept alive to preserve the soil moisture (Personal communication). Also, the frond stack area was usually undisturbed (called death row) and enriched with the organic input from the pruned frond decomposition (Pauli et al., 2014). In contrast, understory vegetation in weeded circles was cleaned up. In the harvesting path, the growth of understory vegetation was consequently depressed because it was stepped on frequently by the harvester. In Jambi, however, farmers sometimes removed understory vegetation even around frond stacks. In both sites, understory vegetation biomass showed a seasonal variation that was dissimilar between Riau and Jambi (Table 7). Different local environments, such as microclimate, soil condition, and canopy cover, have probably affected understory vegetation production. Also, cleaning activity surely influenced biomass production. In this study, understory vegetation production would be underestimated because of weeding. However, the production accounted for 6 and 9% of total ANPP, respectively, in Riau and Jambi, indicating that understory vegetation is not negligible in the NPP of oil palm plantations.

3.3.2. BNPP (including fine root dynamics)

In contrast to ANPP, BNPP was lower in Riau than in Jambi (Table 10). The coarse root NPP was similar between Riau and Jambi because of using the same allometric equation. The result in Riau was slightly higher owing to higher tree density (Table 6). Fine root NPP was larger than coarse root NPP, which accounted for 14 and 21% of total NPP, respectively, in Riau and Jambi (Table 9). The large fine root NPP might have a relation with the structure of the oil palm root system, which has a fast growth but with a limited life span (Jourdan and Rey, 1997). Fine root NPP was lower in Riau than in Jambi, in line with fine root biomass (Tables 8 and 9). Old oil palm plantations on mineral soil generally have higher belowground biomass including fine roots (Syahrinudin, 2005). Hence, the older plantation in Jambi, even on peat soil, is expected to have higher fine root biomass as well as higher fine root NPP (Finér et al., 2011). Furthermore, relatively open areas around the tree bases in Jambi would raise soil temperature, probably resulting in higher fine root NPP than in Riau (Gill and Jackson, 2000; Majdi and öhrvik, 2004).

A significant difference in fine root biomass between at 1 m and 3 m from tree bases (Table 8) was consistent with the previous study, where oil palm root density in peat soil decreased with a distance from tree bases (Dariah et al., 2014). Besides production, studies about fine root mortality and decomposition were also limited in tropical regions (Yuen et al., 2013). In this work, annual C input through root mortality was estimated to be 1.69 and 1.09 (sum of 80% *M* and 20% *S*) Mg C ha^{-1} yr^{-1}, in Riau and Jambi, respectively (Table 9). Fine root decomposition was estimated to be 1.22 and 0.51 (sum of 80% *M* and 20% *S*) Mg C ha^{-1} yr^{-1}, in Riau and Jambi, respectively. The fine root decomposition was 4-11% of total soil respiration (SR) and 7-16% of heterotrophic soil respiration (HR) in oil palm plantations on peat soil (Melling et al., 2005, SR: 15.4, Melling et al., 2013, HR: 693; Dariah et al., 2014, SR: 12.2-13.0, HR: 9.30-10.4; Sakata et al., 2015, SR: 18.2; Ishikura et al., 2018, SR: 10.3, HR: 5.90-6.90 Mg C ha^{-1} yr^{-1}).

3.3.3. Pruned frond decomposition

CO_2 emission through pruned frond decomposition (LD_{frond}) was higher in Riau (1.48) than in Jambi (1.12 Mg C ha^{-1} yr^{-1}). Even for the same cultivar, decomposition rate of *M* was higher in Riau than in Jambi. *S* in Jambi had higher decomposition rate constant (*k*) probably because of a lower CN ratio (Table 4; Khalid et al., 2000; Moradi et al., 2013). The *k* values of *M* in Riau (1.86) and *S* in Jambi (1.81 yr^{-1}; Fig. 12) were similar to a *k* of pruned fronds from oil palm on mineral soil in Malaysia (1.80 yr^{-1}; Moradi et al., 2013). Our annual LD_{frond} in Riau and Jambi accounted for 20 and 15% of soil heterotrophic respiration from oil palm plantations on tropical peatland (Melling et al., 2013; Dariah et al., 2014; Ishikura et al., 2018), accounting for 13% in Riau and 10% in Jambi of a default CO_2 emission factor by Tier 1 methodology for oil palm plantations on peat soil (11 Mg C ha^{-1} yr^{-1}) (IPCC, 2014). Total CO_2 emission from oil palm litter decomposition (LD_{total}), which was roughly estimated as the sum of pruned frond (LD_{frond}) and fine root (LD_{root}) decomposition (1.62-2.69 Mg C ha^{-1} yr^{-1}) accounted for about 20-40% of soil heterotrophic respirations from oil palm plantations on tropical peat (Melling et al., 2013; Dariah et al., 2014; Ishikura et al., 2018).

Total annual C input from pruned fronds and fine root mortality (4.23 and 3.16 Mg C ha^{-1} yr^{-1}, respectively, in Riau and Jambi) were lower than total C input of oil palm litter on mineral soil in Jambi (5.47 Mg C ha^{-1} yr^{-1}), which was a sum of fine root mortality (2.58 Mg C ha^{-1} yr^{-1}) and pruned fronds (2.89 Mg C ha^{-1} yr^{-1}; Kotowska et al., 2016). However, C input from pruned fronds in this study (2.07-2.54 Mg C ha^{-1} yr^{-1}) was higher than that of 1.33-1.79 Mg C ha^{-1} yr^{-1} in an oil palm plantation on

mineral soil in North Sumatra, Indonesia (Lamade and Bouillet, 2005). Compared to C emission, our annual C input (pruned fronds and fine root mortality) was lower than that of soil heterotrophic respiration from oil palm plantations on peat soil (Melling et al., 2013: 6.93 Mg C ha^{-1} yr^{-1}; Dariah et al., 2014: 9.3-10.42 Mg C ha^{-1} yr^{-1}; Ishikura et al., 2018: 6.9 Mg C ha^{-1} yr^{-1}).

3.3.4. Comparison with other oil palm plantations and tropical ecosystems

Two studies were found on the NPP of oil palm plantations on tropical peat, which were conducted in smallholders' young plantations (Melling et al., 2008; Basuki et al., 2018). Our annual NPP of 17.3 and 13.5 Mg C ha^{-1} yr^{-1} were higher than 12.0 Mg C ha^{-1} yr^{-1} of a 5-year-old oil palm plantation in Sarawak, Malaysia (Melling et al., 2008) and much higher than 3.7 Mg C ha^{-1} yr^{-1} of 2 to 3-year-old plantations in Jambi, Indonesia (Basuki et al., 2018). The latter study did not quantify fruit bunch NPP, because the plantations were immature. Also, both did not measure understory vegetation NPP. In comparison with forests, NPP in this study was higher than that of peat swamp forest in West Kalimantan, Indonesia (13.2 Mg C ha^{-1} yr^{-1}, Basuki et al., 2018) and in Federated States of Micronesia (11.2 Mg C ha^{-1} yr^{-1}, Chimner and Ewel, 2005). Besides, our ANPP of 14.0 and 9.9 Mg C ha^{-1} yr^{-1} in Riau and Jambi, respectively (Table 10), were higher than that of ANPP on degraded peat swamp forest in Central Kalimantan (7.9 Mg C ha^{-1} yr^{-1}, Miyamoto et al., 2016; 7.3 Mg C ha^{-1} yr^{-1}, Saragi-Sasmito et al., 2018). As for understory vegetation NPP, there was no previous study in oil palm plantations on peat.

Our annual NPP were equivalent with those of other oil palm plantations on mineral soil in Jambi (17.3 and 15.1 Mg C ha^{-1} yr^{-1}; Kotowska et al., 2015), whereas the study did not quantify understory vegetation NPP that accounted for 6 to 9% of total NPP in our study. Within five components excluding understory vegetation, NPP components in two sites consist of oil palm tree canopy (1.9 and 2.6), pruned fronds (2.5 and 3.3), fruit bunches (11.5 and 8.5), coarse roots (0.3 and 0.4), and fine roots (1.1 and 0.4 Mg C ha^{-1} yr^{-1}); Kotowska et al., 2015); only pruned frond NPP was identical to our result. The tree canopy NPP of the study was lower, but the fruit production was higher than our study. Their high fruit production was similar to the production data in Indonesia, in which the fruit production of oil palm plantations on mineral soil was higher than that on peat soil (Directorate general of estate crops, Indonesia Ministry of Agriculture, 2017). The dissimilarity between our NPP and their NPP is probably because of different methods (including different allometric equations), different age of plantations (their oil palm ages varied between 8 and 15 years old), different tree densities (not mentioned in their study), and different local

environments. Their fine root NPP measured by the ingrowth core method was much lower (0.4-1.1 Mg C $ha^{-1}yr^{-1}$ and 3-6% of total NPP) than our study (2.45-2.86 Mg C $ha^{-1}yr^{-1}$ and 14-21% of total NPP); their results seem to underestimate because sampling intervals were relatively too long (8-10 months). However, our NPP was higher than that (8.14 Mg C ha^{-1} yr^{-1}) of oil palm plantations in Peninsular Malaysia, which was estimated using satellite remote sensing data (Tan et al., 2014). The smaller NPP was probably because of high variation of oil palm tree ages in a wide area of plantations. Also, their C content from a reference of 45% for all oil palm components was smaller than our study (Table 4).

This chapter is submitted as:
Wakhid, N., Hirano, T., Agus, F., Dariah, A., 2020. Net primary production and CO_2 emission from frond decomposition in oil palm plantations on tropical peat.

Chapter 4. Soil CO_2 emissions and net primary production (NPP) of an oil palm plantation on peat in South Kalimantan

4.1. Material and methods

4.1.1. Study site

The study was conducted in a 6-year-old smallholder oil palm plantation on tropical peat located about 30 km southeast of Banjarmasin, the capital city of South Kalimantan, Indonesia (3°24'19.0" S, 114°46'11" E). The peat depth was 6 m on average. The study site was originally shrubland without proper drainage, which was opened for some agricultural land use except oil palm. Surface peat was mostly fibric to hemic. Totally, about 12 ha of peatland was used for oil palm plantations, which was surrounded by farmlands mostly for seasonal vegetables. Oil palm trees were planted in 2013 on a triangular pattern spacing 8 m between trees with a tree density of 147 trees ha^{-1}. Also, two canals (2.5 m of wide) separated by 5 m wide of road were built across the plantation during the field opening. Most of the oil palm trees were leaning because no artificial compaction was made. Compound chemical fertilizer was applied within 1 m around tree bases, which was equivalent to 70 kg N ha^{-1}, 70 kg P_2O_5 ha^{-1}, 70 kg K_2O ha^{-1}, 2 kg MgO ha^{-1}, and 26 kg CaO ha^{-1}. In 2017, organic (manure) fertilizer was also applied at rates of 50 kg for each tree.

4.1.2. Soil CO_2 efflux measurement

Soil CO_2 efflux was measured monthly from September 2018 to March 2020 using a closed chamber system on chamber bases. The chamber was made of opaque PVC with 30 cm in diameter and 20 cm in height. A portable infrared CO_2 analyzer (GMP343, Vaisala, Helsinki, Finland) and a DC data logger (LR 5042, HIOKI, Nagano, Japan) were installed into the chamber system. The CO_2 analyzer was operated in an open-path mode by removing its air filter to improve its time response. Air temperature and CO_2 concentration in chamber headspace were measured every 10 seconds for three minutes on each chamber base. Simultaneously, soil temperature was measured at a depth of 5 cm using a thermometer near chamber bases. The measurement was conducted once in the morning (08:00-11:00) on each day. Soil CO_2 efflux was calculated from air temperature (T_a, ºC) and an increasing rate of CO_2 concentration (dC/dt, μmol m^{-2} s^{-1}) using the equation (1). Also, a linearity test was applied to control the quality of dC/dt following Aguilos et al. (2013). Further information was described in 2.1.3.

To exclude root respiration (RR) and directly measure peat decomposition (PD), soil CO_2 efflux was measured on different distances from tree bases. Roots of oil palm are expected to be relatively localized around each tree, and root density would depend on the distance from tree bases. Thus, chamber bases were categorized into two positions: near (1m, in root circles (RC)) and far (> 3 m). Soil CO_2 efflux at the far positions can correspond to PD, because RR was reported to be negligible (Dariah et al., 2014; Ishikura et al., 2018; Manning et al., 2019). In contrast, soil CO_2 efflux at the near positions correspond to total soil respiration (SR). Besides, to estimate the effect of management, far bases were installed on two different areas: (1) frond stacks (FS), inter-row for pruned frond heap with rich organic material, and (2) harvesting paths (HP) associated with high soil compaction. Before monthly measurement, palm litter or pruned fronds were removed from chamber bases to exclude CO_2 emissions through pruned frond decomposition. Thus, the difference between SR and PD is equivalent to RR. Three bases were installed in RC, FS and HP, respectively. Along with the chamber measurement, ground subsidence (cm yr^{-1}) was also estimated from temporal change in peat surface elevation, using pipes inserted vertically into peat and anchored firmly at underlying mineral substrate (Fig. 13).

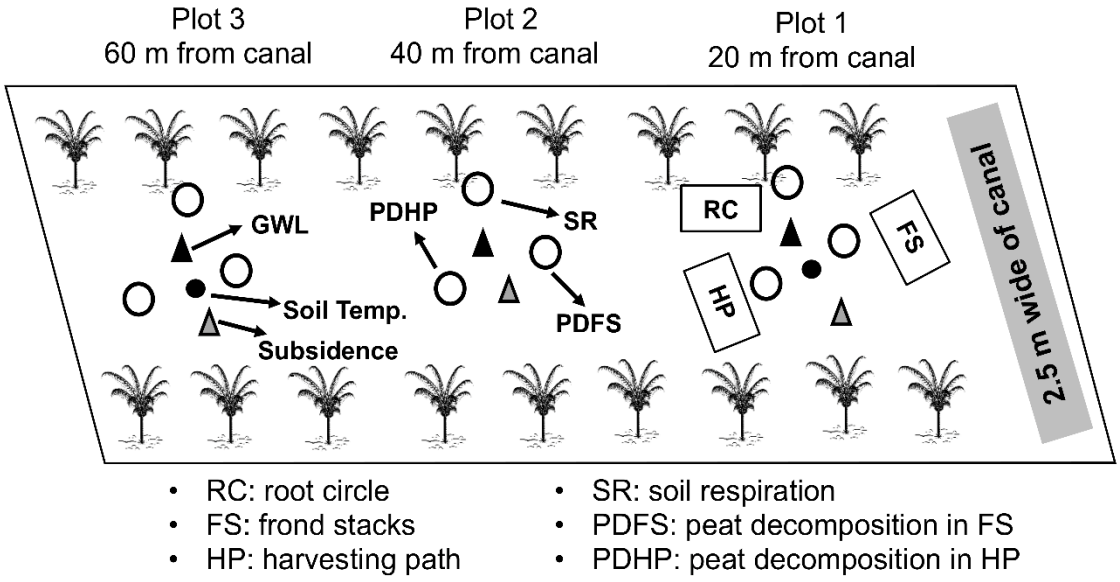

Fig. 13. Experimental plots and the distribution of chamber bases and ground sensors in South Kalimantan.

4.1.3. Litter/ frond decomposition

Frond decomposition was measured using litter bags of 40 cm x 80 cm, which were made of plastic mosquito netting with a mesh size of 2 mm. Fresh old fronds

were used in this experiment following the practical management in oil palm plantation which commonly cut the old frond during fruit harvesting or periodical pruning. Due to big size, a frond was separated into two parts (tip and base) immediately after cutting down. In total, 24 bags were prepared for each of tips and bases and set on the top of frond stacks around chamber plots in September 2018. Six bags were retrieved every two months, November 2018, January 2019, March 2019, May 2019, July 2019, September 2019, November 2019, and January 2020. After retrieved, each of litterbag was carefully cleaned to remove external materials, such as soil and litter particles. Dry weight and carbon (C) content were measured for each retrieved sample. Dry weight was measured by oven-drying at 70°C for at least 48 hours, and C content was determined by the loss of ignition (LoI) method at 550°C in a muffle furnace (Thermolyne type 48000, USA) with a conversion factor of 0.58 from organic matter to organic C (Agus et al., 2011). After July 2019, the C content was unmeasured, because it was almost the same from November 2018 to July 2019; frond C content was assumed to be constant. Also, initial values of dry weight and C content of leaves and rachis were measured at the beginning (n = 3). Decomposition rate constant (k) was estimated by fitting a negative exponential equation to the residual ratio of C amount and elapsed time. Using the k value and initial C amount, C loss through the decomposition of pruned fronds was estimated. Area-based CO_2 emission due to frond decomposition was calculated monthly, then summed up annually using pruned frond production. C loss was assumed to be caused by oxidative decomposition. Detail method for CO_2 emission through pruned frond decomposition (LD_{frond}) estimation was similar to in Riau and Jambi (Chapter 3).

4.1.4. Net primary production (NPP)

NPP (Mg C ha^{-1} yr^{-1}) was defined as biomass production that estimated as a sum of above- and belowground NPP (ANPP and BNPP). ANPP was estimated as a sum of tree canopy (trunks and attached fronds), pruned fronds, and fruit bunch production. Tree canopy NPP was calculated as a cumulative biomass increment (mass difference) between August 2018 and July 2019 using an allometric equation from tree height (Khasanah et al., 2015; equation 3). H was measured in August 2018 and July 2019 for 30 trees, which corresponded to 20% of tree density.

Annual fruit bunch NPP was counted using data recorded by the farmer. Dry weight and C content of fruit bunch were used the same data from Riau (Chapter 3). A frond attached just under a fruit bunch is pruned when the fruit bunch is harvested, and the pruned frond is left on the ground to recover the nutrients from the frond. The fruit production was less because the oil palm trees were young and have been in the

initial stage of fruit production. On average, one frond was pruned nearly bimonthly from one tree. The dry weight and C content of a whole frond were measured. Understory vegetation biomass was measured by destructive sampling from three quadrats of 0.5 m × 0.5 m in three management areas: RC, FS and HP (nine quadrats totally). Understory vegetation was harvested in September 2018, February 2019, and June 2019. Annual NPP of understory vegetation was calculated as a difference between maximum and minimum biomass of each sampling (Scurlock et al., 2002).

BNPP was calculated from the production of coarse and fine roots biomass. Coarse root biomass was calculated using the empirical equation (Syahrinudin, 2005, equation 4). This equation was developed for an oil palm plantation on mineral soil with a density of 140 trees ha^{-1}. Thus, to adjust the tree densities (147 trees ha^{-1}), biomass was scaled with a factor of 1.05 (147 / 140). Annual coarse root NPP was calculated as an annual biomass increase. C content of fine roots measured in Riau (Chapter 3) was used for coarse root NPP calculation. Fine root NPP (≤ 2 mm in diameter) was estimated by sequential soil coring for a depth of 0-30 cm using an auger with a diameter of 2.54 cm. Core sampling was conducted bimonthly in September 2018, November 2018, January 2019, March 2019, May 2019, and July 2019 near three trees at different distances from the canal (Fig. 13). For each tree, soil cores were collected at 1, 2, and 3 m distance from the tree base in four directions (Fig. 10). Totally, 12 soil core samples around each tree were collected. Soil cores were stored in plastic bags and washed with tap water to separate roots from peat soil. By sieving, only fine roots of oil palm trees were extracted and then separated into living (biomass) and dead ones (necromass) by visual inspection based on color and shape (Makkonen and Helmisaari, 1999). Fine roots of oil palm trees were rough, rigid, and a little bit dark in color, whereas roots of understory vegetation were distinguished by their light color, and soft without a lignified periderm (Leuschner et al., 2009). Fine root production, mortality, and decomposition between sampling dates were estimated by a simplified decision matrix method (Yuan and Chen, 2013), and annual fine root NPP was calculated as the sum of production. Detail method for NPP measurement was similar to in Riau and Jambi (Chapter 3).

4.1.5. Soil environment

To analyze soil C and N contents, nine peat samples were collected on September 2018, at three management areas (RC, HP, and FS) from 0 to 30 cm. C content was determined by the loss of ignition (LoI) method at 550°C in a muffle furnace (Thermolyne type 48000, USA) with a conversion factor of 0.58 from organic matter to organic C. While, N content was determined with the Kjeldahl technique.

Bulk density (BD) was analyzed from peat samples collected in 0-50, 50-100, 100-150, and 150-200 cm from three plots in the dry season (August, 2018), when the groundwater level (GWL) was low. Peat samples were taken using peat auger (Eijkelkamp, Netherland) following Agus et al. (2011), because peat soil maturity was low. Peat BD was estimated using gravimetric method in the laboratory. GWL was measured hourly at three plots (Fig. 13) using water pressure sensors (Model HTV 050KP-10-V, Sensez Co., Tokyo, Japan in plot 1 and 3; and HOBO U20-001-01, Onset computer, USA, in plot 2) in a perforated PVC pipe inserted vertically deep into mineral soil. GWL was also measured manually once a month in accordance with soil CO_2 efflux measurement. Soil temperature was recorded hourly using a small temperature data logger (Thermochron SL type, KN laboratories, Osaka, Japan) installed at a depth of 5 cm in plot 1 and 3 near the pipes for GWL measurement.

4.1.6. Statistical analysis

Differences among the treatment or components were analyzed using analysis of variance, and specific differences among groups were analyzed using Tukey's multiple comparison test. The correlation between soil CO_2 and environmental factors was analyzed using Pearson correlation method. All data analysis was conducted using R software (R Development Core Team 2019; version 3.5.3).

4.2. Results

4.2.1. Oil palm component characteristic

The initial C content of pruned fronds was averaged at 55.4 ± 1.83 % (mean ± 1 SD, n =3). C contents were not significantly different between tip and base parts, but significantly different between leaves and rachis (Table 11). The initial C content of understory vegetation in all management areas was 51.8 ± 6.06 % (mean ± 1 SD, n = 3).

4.2.2. Soil environmental factors

Peat soil C content was not significantly different between RC, FS, and HP (p > 0.05; Table 12). Mean BD from 3 plots was 0.14 ± 0.04, 0.12 ± 0.04, 0.11 ± 0.03, and 0.17 ± 0.05 g cm^{-3} at a depth of 0-50, 50-100, 100-150, and 150-200 cm, respectively (n = 3). In 2019, the dry season which defined as the months with precipitation less than 100 mm $month^{-1}$ (Hirano et al., 2015) was from June through October (Fig. 14a). Mean daily soil temperature ranged from 26 to 33 °C in plot 1 and 27 to 32 °C in plot 3 during the flux measurement period. Unfortunately, soil

temperature data were missing from July to August because of a sensor problem (Fig. 14b). Mean annual GWL using automatic loggers from three plots was -0.75 ± 0.09 m from September 2018 to September 2019. GWL varied seasonally between -1.49 and 0.15 m in plot 1, between -1.36 and 0.01 m in plot 2, and between -1.36 and 0.02 in plot 3 (Fig. 14d). Using monthly manual records during the CO_2 efflux measurement, temporal variation of GWL varied between -0.39 and -1.28 m with an average of -0.74 m (Fig. 14c). GWL was high in the wet season from December to June and low in the dry season from July to November following a seasonal variation in precipitation (Fig. 14 a, c, & d). After September 2019 the automatic GWL sensors were broken in plots 1 and 3. Also, the GWL sensor in plot 2 was lost. GWL was significantly different between plot 1, 2, and 3 from automatic measurement, but not significantly different between the three plots from monthly manual records. GWL from monthly manual was not significantly different from automatic on the same day during the CO_2 efflux measurement ($P > 0.05$).

Table 11. Initial amount of carbon (C, $n = 3$) and water content (WC, $n = 5$) of frond (mean ± 1 SD).

Samples	C (%)	WC (%)
Dry weight = 1539 ± 298 g frond^{-1}, $n = 5$)		
Leaf (tip)	53.4 ± 0.37	69.1 ± 4.11
Rachis (tip)	57.0 ± 0.05	76.3 ± 5.54
Leaf (base)	54.2 ± 1.43	75.0 ± 3.54
Rachis (base)	57.0 ± 0.78	63.3 ± 9.07
ANOVA (P value)		
Component (leaf vs. rachis)	<0.001	0.71
Position (tip vs. base)	0.43	0.93
Interaction (component-position)	0.42	<0.001

Table 12. Main characteristics of peat (mean ± SD, $n = 3$).

Area	BD (0-50 cm of depth, g cm^{-3})	C content (%)	N content (%)	C/N
Root circle (RC)	0.14 ± 0.04	48.5 ± 2.62	1.24 ± 0.39	43.1 ± 18.9
Harvesting path (HP)		50.0 ± 0.18	0.81 ± 0.10	62.1 ± 8.10
Frond stack (FS)		45.9 ± 5.56	1.01 ± 0.22	45.9 ± 4.25
ANOVA (P value)				
Area		0.43	0.23	

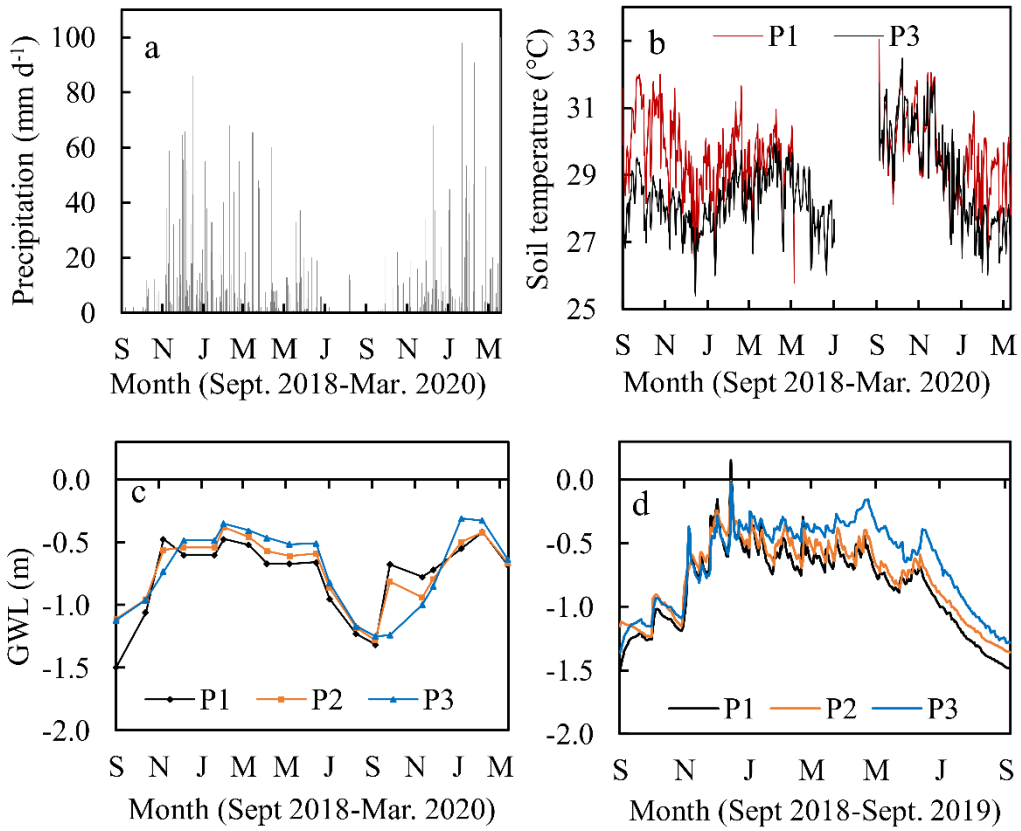

Fig. 14. Variations in daily values of (a) precipitation, (b) soil temperature in plot 1 and 3, (c) groundwater level (GWL) in 3 plots from monthly manual measurement from September 2018 to March 2020, and (d) GWL from automatic measurement in 3 plots from September 2018 to September 2019 (data after September 2019 were missing because of the sensors problem). Precipitation was measured about 5 km distant from the study site (BMKG, South Kalimantan).

4.2.3. Soil CO_2 efflux

In total, 96% of CO_2 efflux data were available after quality control. Mean SR (in RC) from three plots showed small seasonal variation from 4.0 µmol m^{-2} s^{-1} in June 2019 to 10.6 µmol m^{-2} s^{-1} in September 2018. Although seasonal variation was small, SR was generally higher when GWL was lower (Figs. 14c, d, and 15a). Vague seasonal variation was also found in PD both in FS and HP (PDFS and PDHP; Fig. 15b). The highest SR and mean PD was measured in September 2018, a month with the lowest GWL during CO_2 efflux measurement in 2018 and 2019 (-1.24 and -1.28 m, respectively; Figs. 14c and 15a, b). Mean SR from 3 plots was significantly larger ($p < 0.001$) than those of PDFS and PDHP (Table 13), though there was no significant difference between PDFS and PDHP ($p > 0.05$).

Both PD showed a significant relationship with GWL ($p < 0.05$, Fig. 16), but no in SR. Also, there was no significant relationship between SR or PD and soil temperature ($p > 0.05$, data not shown). Annual SR and PD were simply estimated as a mean of monthly measurements because their seasonal variations were small (Fig. 15). Annual SR was estimated to be 23.1 Mg C ha^{-1} yr^{-1}, whereas annual mean PD from FS and HP was 15.4 Mg C ha^{-1} yr^{-1}. The difference between SR and PD was 7.70 Mg C ha^{-1} yr^{-1}, which nearly corresponds to annual root respiration (RR). PD accounted for 67% of SR on an annual basis.

Table 13. Mean soil CO_2 efflux on different management areas (mean ± SD; $n = 3$) from September 2018 to March 2020. Different alphabets in the CO_2 emission from mean efflux denote significant difference ($P < 0.05$) between management area (RC, FS, and HP) according to Tukey HSD test after ANOVA.

Position on different management area	CO_2 efflux (μ mol CO_2 m^{-2} s^{-1})	Annual CO_2 emissions from mean efflux (Mg C ha^{-1} yr^{-1})
Near the tree base in the root circle (RC): correspond to SR	5.09 ± 1.62a	23.1 ± 6.13
Far from the tree base in the frond stack (PDFS): correspond to PD	3.88 ± 1.31b	14.7 ± 4.98
Far from the tree base in the harvesting path (PDHP): correspond to PD	4.24 ± 0.97b	16.1 ± 3.69
Mean PD		15.4 ± 4.37
Residual: correspond to RR		7.70 (33% of SR)

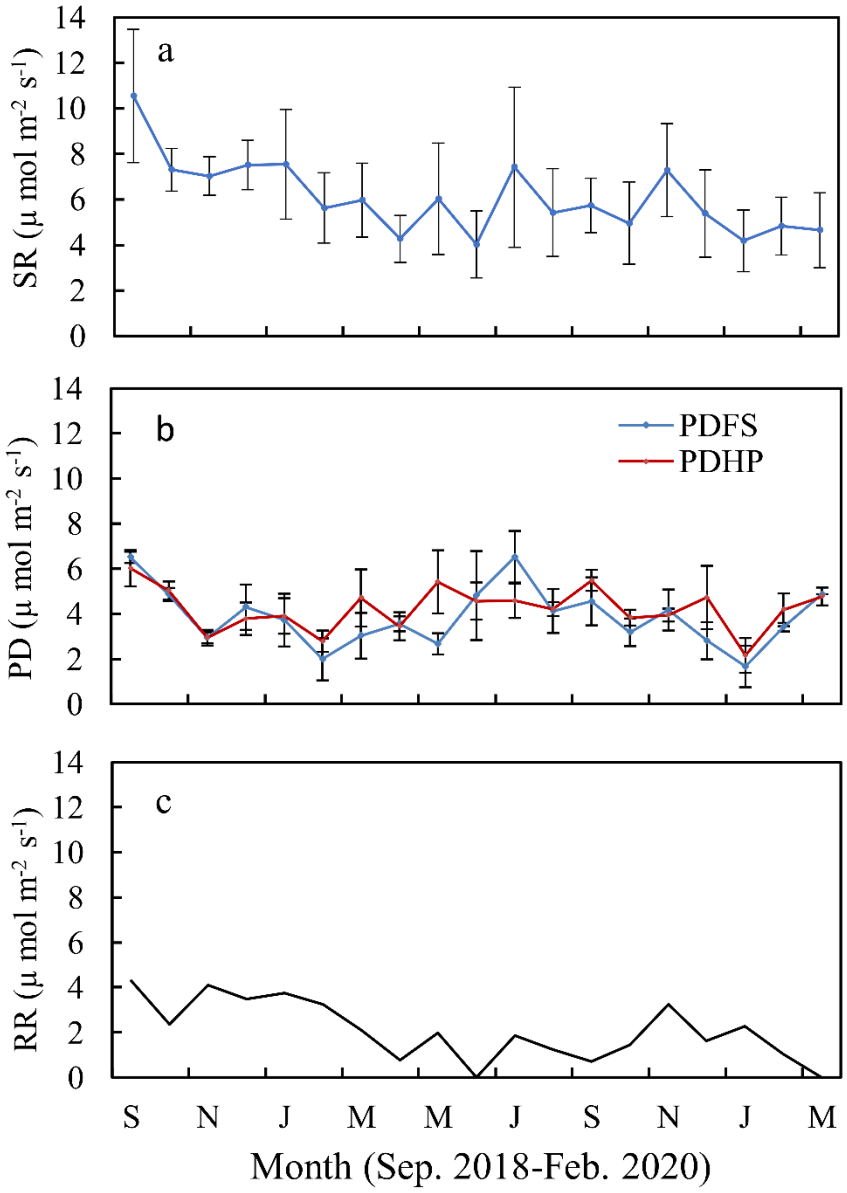

Fig. 15. Mean seasonal variations in (a) total soil respiration (SR, in the root circle (RC) near the tree base, *n* = 3), (b) peat decomposition in the frond stack (PDFS) and the harvesting path (PDHP) from 3 plots (*n* = 3), and (c) residual between means of SR and PD that correspond to root respiration (RR) from September 2018 to March 2020. Vertical bars denote 1 standard error (SE).

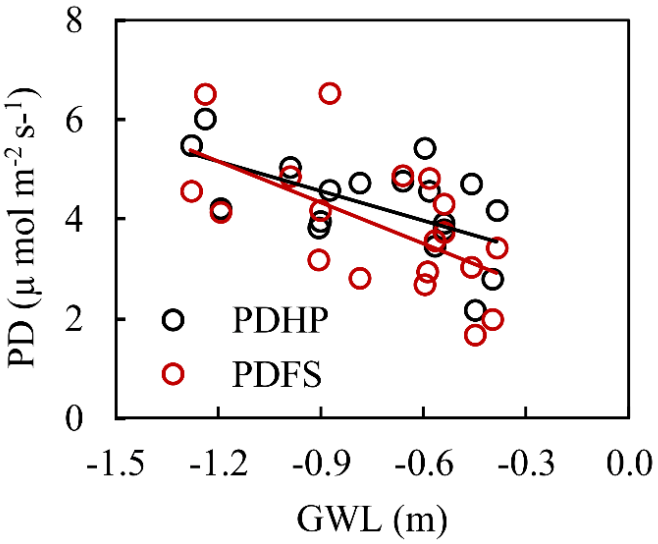

Fig. 16. Relationship between peat decomposition (PD) and groundwater level (GWL) on different management area: peat decomposition in the harvesting path (PDHP, black circle) and peat decomposition in the frond stack (PDFS, red circle). Each symbol denotes an average of 3 plots (n = 3). A line is fitted for each management area (p < 0.01). PDHP: y = -1.99x + 2.77 (r^2 = 0.34), and PDFS: y = -2.78x + 1.84 (r^2 = 0.36).

4.2.4. Peat subsidence

The elevation of the peat surface varied in parallel to GWL from September 2018 to March 2020 (Fig. 17). The variation of peat surface elevation changed after October 2019 at the end of the dry season. After October 2019, elevation did not follow GWL. Peat elevation from October 2018 to September 2019, and from October 2019-March 2020, showed positive significant relationships with GWL (p < 0.001 for until September 2019 and p < 0.01 for after October 2019; Fig. 18). The slopes of the linear relationships were different between the two periods. In the former period, the slope which was an elevation sensitivity to GWL was changed much higher than in the latter periods after the lowest GWL was measured; the slopes were 17.5 and 5.07 cm m^{-1} respectively.

If peat elevation was predominantly affected by GWL, annual subsidence was calculated as a difference in peat elevation in similar GWL conditions. Peat surface elevation relative to the initial value in September 2018 was 0.88 ± 0.33 cm (mean ± 1 SD, n = 3) on February 10, 2019 with GWL of -0.40 m, and -16.5 ± 3.13 cm on

February 14, 2020 with GWL of -0.39 m. Because GWL was almost the same, annual subsidence can be simply calculated to be 17.2 ± 3.02 cm yr^{-1}, after adjusting the number of days from 369 to 365 days.

Subsidence due to oxidative peat decomposition was separately calculated from PD values in FS and HP using BD of surface peat (0-50 cm of depth) and C content of surface peat (0-30 cm from different management area; Table 12). As a result, subsidence through PD was estimated to be 2.33 cm yr^{-1} and accounted for 14% of total subsidence of 17.2 cm yr^{-1} (Table 14).

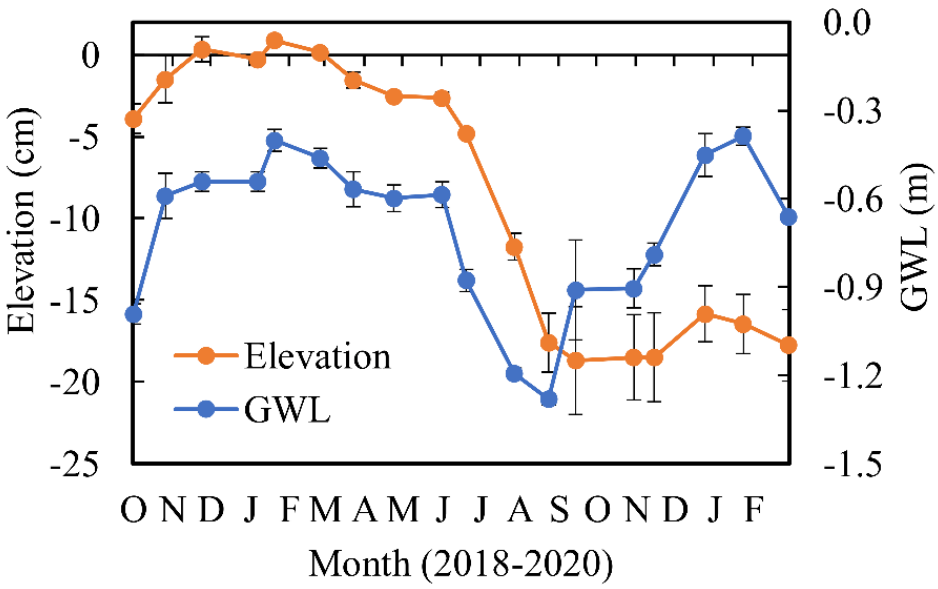

Fig. 17. Seasonal variations in peat surface elevation and groundwater level (GWL) from October 2018 through March 2020. Mean elevation (n = 3) is shown relatively to that in September 2018. Vertical bars denote 1 standard error (SE).

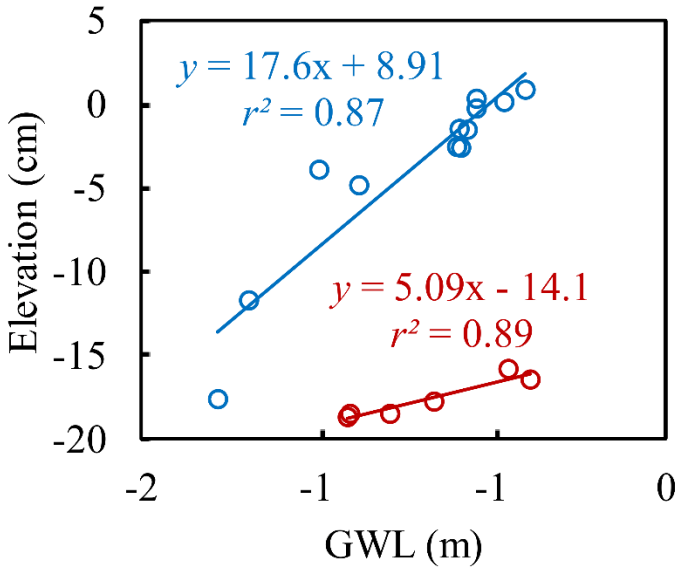

Fig. 18. Relationship between peat elevation and groundwater level (GWL) from October 2018 to September 2019 (blue circle), and October 2019 to March 2020 (red circle). A line was fitted for each period.

Table 14. Annual subsidence through oxidative peat decomposition (PD). Annual PD was converted to annual subsidence using bulk density (BD) 0-50 cm and carbon (C) content of peat 0-30 cm. For BD, C content, and total subsidence, mean ± 1 SD (*n* = 3) is shown.

Periods	Annual PD (Mg C ha^{-1} yr^{-1})	BD (g/cm^3)	C content (%)	Subsidence through PD (PDs, cm yr^{-1})	Total subsidence (cm yr^{-1})	Contribution
Sept 2018-March 2020	14.7	0.14 ± 0.04	48.1 ± 2.04	2.22	17.2 ± 3.02	13%
	16.1			2.43		14%

4.2.5. CO_2 emission through pruned frond decomposition (LD_{frond})

The dry weight of a whole pruned frond was 1539 ± 298 g $frond^{-1}$ (Table 11), and C amount averaged at 863 ± 167 C $frond^{-1}$ (mean ± 1 SD, *n* = 5). The temporal pattern of C loss through pruned frond decomposition followed a negative exponential

(Fig. 19), with a frond decomposition rate constant (*k*) was estimated to be 1.41 yr^{-1}. Using the *k*, the pruned frond was estimated to be decomposed by 90% in 1.67 years. Annual carbon input through pruned fronds into the plantation was estimated to be 0.76 Mg C ha^{-1} yr^{-1} from a calculation that annual input of pruned fronds (6 fronds $tree^{-1}$ yr^{-1}) × dry weight (1539 g $frond^{-1}$) × C content (55.4 %) × tree density (147 trees ha^{-1}), whereas annual CO_2 emission through decomposition was calculated to be 0.38 Mg C ha^{-1} yr^{-1}.

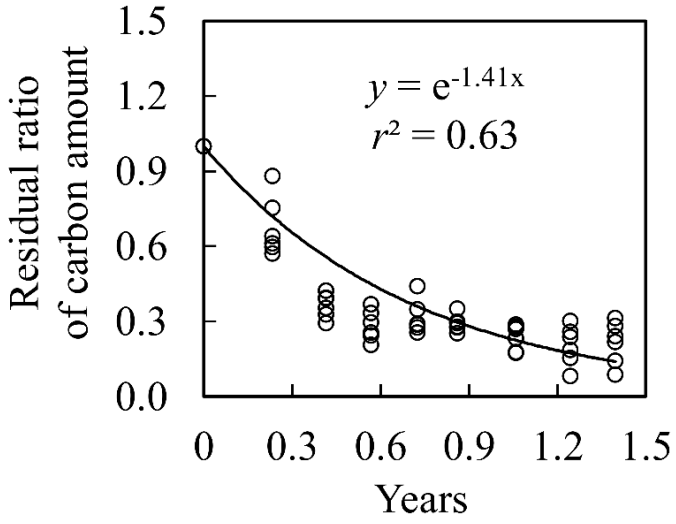

Fig. 19. C loss pattern of pruned fronds.

4.2.6. Net primary production (NPP)

Annual height increment from August 2018 to July 2019 was 0.67 ± 0.20 m $tree^{-1}$ (Table 15). As a result, biomass growth was estimated to be 0.06 ± 0.02 Mg $tree^{-1}$ yr^{-1}. Understory vegetation biomass at three different management areas (RC, FS, and HP) was not significantly different (Table 16). Understory vegetation biomass showed a significant seasonal difference between first and second or second and third samplings. Between the first and third samplings, understory vegetation biomass was not significantly different. Fine root biomass was decreased with distance from tree bases and showed significant seasonality (Table 17). Fine root biomass in July to September was significantly higher than in January to May. Not only biomass, fine root necromass also showed a significant difference between positions and seasons. While, fine root production, mortality, and decomposition showed a significant difference between seasons (Table 18).

Annual total NPP was estimated to be 10.9 Mg C ha^{-1} yr^{-1} (Table 19), which was dominated by ANPP (8.51 Mg C ha^{-1} yr^{-1}, 78%). As a young plantation, fruit production was still low. Therefore, the most contribution to total NPP was from tree canopy production, which accounted for 49%, followed by fruit bunch production with 16% of contribution. Annual BNPP was 2.40 Mg C ha^{-1} yr^{-1}, of which fine root production accounted for 64%.

Table 15. Tree height and canopy biomass (mean ± 1 SD; n = 30) from August 2018 to July 2019.

Component		Oil palm tree canopy
Tree height (m)	August 2018	0.80 ± 0.34
	July 2019	1.47 ± 0.42
Height growth (m yr^{-1})		0.67 ± 0.20
Biomass (Mg $tree^{-1}$)	August 2018	0.17 ± 0.03
	July 2019	0.24 ± 0.04
Biomass growth (Mg $tree^{-1}$ yr^{-1})		0.06 ± 0.02
Tree density (trees ha^{-1})		147
Biomass (Mg ha^{-1})	August 2018	25.0
	July 2019	34.3
Biomass growth (Mg ha^{-1} yr^{-1})		9.29

Table 16. Understory vegetation biomass **(**mean ± 1 SD, n = 3). Different alphabets in the date column mean denote a significant difference (p < 0.05) according to Tukey HSD test after ANOVA.

Area	Biomass (Mg ha^{-1})			
	Aug. 2018	Jan. 2019	Jul. 2019	Mean
Root circle	0.11 ± 0.07	1.53 ± 1.28	0.54 ± 0.56	0.72 ± 0.73
Harvesting path	0.53 ± 0.31	1.29 ± 0.91	0.83 ± 0.99	0.88 ± 0.38
Frond stack	0.36 ± 0.38	2.18 ± 0.97	0.26 ± 0.28	0.94 ± 1.08
Mean	0.33 ± 0.21b	1.67 ± 0.46a	0.54 ± 0.28b	0.85 ± 0.11
ANOVA (p value)				
Area	0.82			
Season	<0.01			
Interaction (area-season)	0.53			

Table 17. Biomass and necromass (Mg ha^{-1}) of fine roots (mean ± 1 SD; $n = 4$). Different alphabets in seasonal mean values denote significant difference at positions ($P < 0.05$) and in positional mean values denote significant difference in seasonal variations ($p < 0.05$), according to Tukey HSD test ($P < 0.05$) after ANOVA.

	Biomass			Necromass			Mean	
	1 m	2 m	3 m	1 m	2 m	3 m	Biomass	Necromass
Sep. 2018	2.17 ± 1.41	1.20 ± 0.96	0.67 ± 0.47	0.91 ± 0.63	0.59 ± 0.81	0.26 ± 0.31	1.35 ± 0.76a	0.59 ± 0.32 (a)
Nov. 2018	1.40 ± 0.50	1.30 ± 0.63	0.66 ± 0.84	0.73 ± 0.70	0.53 ± 0.54	0.44 ± 0.51	1.12 ± 0.40a	0.57 ± 0.15 (a)
Jan. 2019	0.47 ± 0.28	0.23 ± 0.20	0.14 ± 0.14	0.30 ± 0.21	0.15 ± 0.20	0.11 ± 0.15	0.28 ± 0.17b	0.19 ± 0.10 (b)
Mar. 2019	0.43 ± 0.53	0.37 ± 0.64	0.14 ± 0.19	1.05 ± 0.84	0.45 ± 0.33	0.18 ± 0.28	0.31± 0.16b	0.56 ± 0.44 (a)
May 2019	0.37 ± 0.43	0.22 ± 0.28	0.29 ± 0.31	0.70 ± 0.32	0.37 ± 0.29	0.44 ± 0.58	0.29 ± 0.08b	0.50 ± 0.17 (ab)
Jul. 2019	1.89 ± 1.70	1.11 ± 0.94	0.36 ± 0.33	1.14 ± 0.85	0.46 ± 0.46	0.41 ± 0.43	1.12 ± 0.76a	0.67 ± 0.41 (a)
Mean	1.12 ± 0.80 (a)	0.74 ± 0.52 (b)	0.38 ± 0.24 (c)	0.81 ± 0.59a	0.42 ± 0.32b	0.31 ± 0.25b		
ANOVA (p value)	Biomass	Necromass						
Position	< 0.001	< 0.01						
Season	< 0.001	< 0.01						
Interaction position-season	< 0.05	0.75						

Table 18. Fine root production (NPP), mortality, and decomposition (mean ± 1 SD; *n* = 12) from September 2018 to July 2019. Lower case letters indicate significant difference in seasonal production, mortality, and decomposition according to Tukey HSD test ($p < 0.05$) after ANOVA. Data of fine root production, mortality, and decomposition on different distances from the tree base were not shown.

Site	Mg C ha^{-1}		
	Production (NPP)	Mortality	Decomposition
Sept.-Nov.	0.34 ± 0.54b	0.47 ± 0.49ab	0.48 ± 0.63ab
Nov.-Jan.	0.01 ± 0.05b	0.49 ± 0.05a	0.71 ± 0.62a
Jan.-March	0.31 ± 0.47b	0.29 ± 0.34bc	0.08 ± 0.16c
March-May	0.19 ± 0.33b	0.21 ± 0.28c	0.24 ± 0.43bc
May-July	0.68 ± 0.77a	0.21 ± 0.31c	0.11 ± 0.22c
Annual	1.53 ± 1.06	1.66 ± 0.88	1.62 ± 0.91
ANOVA (*p* value)			
Season	<0.001	<0.001	<0.001
Positions	<0.05	<0.001	<0.05
Interaction position-season	<0.05	0.08	0.07

Table 19. Net primary production (NPP) based on biomass and carbon.

Component	NPP based on Biomass (Mg ha^{-1} yr^{-1})	NPP based on Carbon (Mg C $ha^{-1}yr^{-1}$)
Aboveground NPP (ANPP)		
Tree canopy	9.29	5.30
Pruned frond	1.36	0.76
Fruit bunch	3.00	1.73
Understory vegetation	1.34	0.72
Total	15.0	8.51
Belowground NPP (BNPP)		
Coarse root	1.52	0.86
Fine root	2.70	1.53
Total	4.23	2.40
Total NPP (ANPP + BNPP)	19.2	10.9

4.3. Discussion

4.3.1. Soil CO_2 emissions

GWL has been reported to mainly control PD in various land uses on tropical peatland (Acacia, Jauhiainen et al., 2012; Forest, Itoh et al., 2017; Oil Palm, Ishikura

et al., 2018). Similarly, in this site, a significant negative relationship between PD and GWL was found even with a low coefficient of determination (Fig. 16). In a compacted rubber plantation (Chapter 2), a strong relationship was found between PD and GWL in an El Niño year with the lowest GWL down to −1.71 m. In this site, the lowest GWL was -1.49 m, which was 0.22 m higher than that in the rubber plantation. SR was not significantly correlated with GWL. No significant relationship between SR and GWL was likely due to the small seasonal variation of RR as the difference of SR to PD. Moreover, there was no significant relationship between SR or PD to soil temperature. Weak relationship to soil temperature might be due to the small amplitude of soil temperature on an annual basis (Fig. 14b).

SR was significantly higher than both of PD, which suggested that PD was low or even free from RR contribution. This result was in line with those of previous studies in oil palm plantations on peat soil, which found RR far from tree bases was mostly negligible (Dariah et al., 2014; Ishikura et al., 2018; Manning et al.; 2019). RR as the residual of SR from PD decreased in the early dry season (Fig. 15c), when GWL began to lower (Fig. 14c, d). This phenomenon suggested root growth was probably depressed in the dry season. Even showed only small seasonality, the variation of RR was in line with the fine root mortality estimation which decreased from March to July 2019 (early dry season) and increased again in July to September 2019 (end of the dry season, Table 18).

Annual soil CO_2 emissions were calculated by averaging periodic CO_2 flux measurement using data for more than one year because the seasonal variation of CO_2 efflux was small. The annual PD of 15.4 Mg C ha^{-1} yr^{-1} was in the range of IPCC default CO_2 emission factor for oil palm plantation on tropical peat (11.0 Mg C ha^{-1} yr^{-1} with 95% confidence intervals or 5.60–17.0 Mg C ha^{-1} yr^{-1}). PD in this site was higher than those of young oil palm plantations (4-7 years old) on peat in Sarawak, Malaysia, Jambi, and Central Kalimantan, Indonesia (Melling et al., 2013, 4 years old, 6.93 Mg C ha^{-1} yr^{-1}, GWL: -0.58 m; Dariah et al., 2014, 6 years old, 10.4 Mg C ha^{-1} yr^{-1}, GWL: -0.52 m; Hergoualc'h et al., 2017, 6 years old, 8.40 Mg C ha^{-1} yr^{-1}, GWL: -0.34 to -0.45 m). The higher PD in this study may have been caused by the lower GWL with a mean of -0.74 m. However, our PD was lower than those of oil palm plantations in Riau, Indonesia (Husnain et al., 2014, 4 years old, 18.0 Mg C ha^{-1} yr^{-1}, GWL: -0.72; Comeau et al., 2016, 7 years old, 18.4 Mg C ha^{-1} yr^{-1}, GWL: -0.78).

PD accounted for 67% of SR (23.1 Mg C ha^{-1} yr^{-1}) on an annual basis (Table 13). The contribution of PD was similar to Hergoualc'h et al. (2017; 61% of 13.8 Mg C ha^{-1} yr^{-1}), but lower than that of Dariah et al. (2014; 85% of 12.2 Mg C ha^{-1} yr^{-1}), and higher than that of Melling et al. (2013; 38% of 18.1 Mg C ha^{-1} yr^{-1}). RR in this

site (7.70 Mg C ha^{-1} yr^{-1}) was higher than RR of young oil palm plantations in Jambi and Central Kalimantan, Indonesia, respectively (1.78 Mg C ha^{-1} yr^{-1}, Dariah et al., 2014; 3.60-5.40 Mg C ha^{-1} yr^{-1}, Hergoualc'h et al., 2017), but lower than RR of a young oil palm plantation in Malaysia (11.2 Mg C ha^{-1} yr^{-1}, Melling et al., 2013).

An annual subsidence rate of 17.2 ± 3.02 cm yr^{-1} was found from the difference in peat surface elevation in the same GWL condition. The annual subsidence in this site was much higher than 3.9 cm yr^{-1} in a 5-year-old oil palm plantation on peat in Jambi, 7 years since drainage (Couwenberg and Hooijer, 2013) and 4.7 cm yr^{-1} in a 1-year-old oil palm plantation in Jambi, 1 year after drainage (Khasanah and Noordwijk, 2018). However, the latter plantation was experienced been logged many years ago. Our result was similar to that of Hooijer et al. (2012), who reported that the subsidence of acacia plantations in the second and third year after drainage was 19 cm yr^{-1} and that the subsidence was stabilized at around 5 cm yr^{-1} at six years after drainage. This plantation was about 6 years old after initial drainage with the mean annual GWL of -0.74 m. Prior to the plantation, this field was a grassland without physical compaction during land preparation. Therefore, the high subsidence in this site may be due to the process of peat consolidation, compaction, and shrinkage that are likely progressing until today.

Subsidence due to the oxidative peat decomposition (PDs) from annual PD was 2.33 cm yr^{-1}, which accounted for 14% of total subsidence. This contribution was lower than those of oil palm and acacia plantations over 5 years after drainage with an average contribution of 75% with PDs of 3.25 cm yr^{-1} (Hooijer et al., 2012). PDs in this site was higher than a peat compacted rubber plantation in Central Kalimantan that found a PDs of 1.50 cm, but with a higher contribution to total subsidence of 25% (Chapter 2). This difference was attributable to the high variation of annual total subsidence which much higher in this site. Also, PDs was influenced by peat BD and C content (Hooijer et al., 2012; Couwenberg and Hooijer, 2013). With the same rate of subsidence, lower BD and C content would be resulting in a lower PD.

4.3.2. Litter decomposition (LD) and total soil respiration (SR_{tot})

CO_2 emission through pruned frond decomposition (LD_{frond}) was estimated to be 0.38 Mg C ha^{-1} yr^{-1}, which contributed 2.4 % to PD. LD_{frond} depended on *k* value and frond production. As an artificial pruning, pruned frond production was varied between plantations depends on the farmer or company activity. LD_{frond} in South Kalimantan was 1/3 and 1/4 of LD_{frond} in Jambi and Riau, respectively (1.12 and 1.48 Mg C ha^{-1} yr^{-1}, in Jambi and Riau, respectively; Chapter 3). Also, *k* value in this site (1.41) was lower than those in Riau (1.86) and Jambi (1.81), respectively. *k* value in

this site was lower than that in an oil palm plantation on mineral soil in Malaysia (1.80 yr^{-1}; Moradi et al., 2014).

This study also estimated the decomposition of belowground litter (fine root, LD_{root}) that estimated to be 1.62 Mg C ha^{-1} yr^{-1} (Table 18), higher than LD_{frond}. However, as an integrated process of fine root production, mortality, and decomposition, LD_{root} mostly included in RR as the difference between PD and SR. Therefore, total soil respiration (SR_{tot} = SR (PD+RR) + LD_{frond}) was estimated at 23.5 Mg C ha^{-1} yr^{-1} (PD: 15.4, RR: 7.70, including 1.62 of LD_{root}, and LD_{frond}: 0.38).

4.3.3. Net primary production (NPP)

NPP in this study (10.9 Mg C ha^{-1} yr^{-1}) was lower than in a 5-year-old oil palm plantation Malaysia (12.0 Mg C ha^{-1} yr^{-1}; Melling et al., 2008), though that study did not estimate the NPP from understory vegetation. NPP in this site was also lower than those of NPP in mature oil palm plantations on peat soil in Riau (17.3) and Jambi (13.5) Mg C ha^{-1} yr^{-1}, respectively (Chapter 3), or on mineral soil in Jambi (17.3 and 15.1 Mg C ha^{-1} yr^{-1}, Kotowska et al., 2015). However, our result was much higher than that of 2 to 3 years old smallholder oil palm plantations on peat in Jambi (3.70 Mg C ha^{-1} yr^{-1}, Basuki et al., 2018), but they did not measure the NPP from palm fruit because the plantations were immature. NPP of oil palm plantation most likely depended on the age of oil palm trees. Mature oil palm plantations tend to have higher NPP than young plantations.

Fruit production contributed most to NPP of mature oil palm plantations in Riau and Jambi (Chapter 3), but in this site, the most contribution was from tree canopy production (Table 19). Oil palm tree begins to produce 3 or 4 years after planted (Corley and Tinker, 2003). Therefore, as 6 years old, the fruit production in this site is still under developing. Also, as a smallholder plantation on peat soil, fruit production was typically lower than in industrial plantations or plantations on mineral soil (Directorate general of estate crops, Indonesia Ministry of Agriculture, 2017).

Fine root NPP in this site (1.53) was lower than those in Jambi (2.86) and Riau (2.45 Mg C ha^{-1} yr^{-1}), respectively (Chapter 2). Fine root NPP most likely depends on the palm age (Syahrinudin, 2005; Finér et al., 2011). Although, air temperature was also found to affect the fine root production in oil palm plantations on mineral soil (Violita et al., 2016). Furthermore, the nutritional and water necessity of mature oil palm plantations were higher than that of young plantations (Corley and Tinker, 2003). Thus, as a key role for nutrition and water uptake, fine root NPP of mature plantations should be higher than in young plantations. Older oil palm trees on mineral soil were reported having higher root density with higher water uptake (Safitri et al., 2019).

4.3.4. Carbon (C) emission through heterotrophic respiration (HR) versus C sequestration through net primary production (NPP)

HR has reported being appointed as a major source of C loss and key component of the soil C balance in tropical peatlands (Hergoualc'h and Verchot, 2013). However, most studies commonly separated the total soil respiration (SR) with root respiration (RR) to heterotrophic respiration (HR) or peat decomposition (PD) without measure the litter decomposition (LD) as a part of heterotrophic respiration (Jauhiainen et al., 2012; Hergoualc'h and Verchot, 2013; Hergoualc'h et al., 2017). In this study, HR was estimated as a sum of PD and LD_{frond} to be 15.8 Mg C ha^{-1} yr^{-1} (15.4 + 0.38 Mg C ha^{-1} yr^{-1}). The contribution of LD_{frond} was small but would be larger in line with the production growth of oil palm trees.

In contrast to emission, we also studied carbon sequestration through net primary production (NPP), defined as total biomass production over a given interval as a result of plant photosynthesis (Clark et al., 2001). Total NPP in this site (10.9 Mg C ha^{-1} yr^{-1}, Table 19) was lower than that of HR (15.8 Mg C ha^{-1} yr^{-1}). As a result, if only from these two-contrast carbon effluxes comparison, the oil palm plantation in this site was acted as a CO_2 source (negative C balance). The net C source of -4.9 Mg C ha^{-1} yr^{-1} (= NPP – HR) in this site was a bit higher than that of net C source of -2.01 Mg C ha^{-1} yr^{-1} from a 5-year-old oil palm plantation in Malaysia (Melling et al., 2008).

This chapter is under preparation for submission as
Wakhid, N., Hirano, T., 2020. Soil CO_2 emissions and net primary production of an oil palm plantation on 6 m depth of tropical peat.

Chapter 5. General discussion

5.1. Soil CO_2 emissions including litter decomposition of agricultural plantations on peat soil

This study showed soil CO_2 emission through PD from two main agricultural plantations on peat soil in Indonesia, rubber and oil palm plantations (Chapters 2 and 4). PD was mostly controlled by GWL both in rubber and oil palm plantations. PD in a rubber plantation in Central Kalimantan was 14.1 Mg C ha^{-1} yr^{-1} with mean GWL of -0.69 m. Whereas in an oil palm plantation in South Kalimantan, PD was 15.4 Mg C ha^{-1} yr^{-1}, with mean GWL of -0.74 m. The results in both plantations were similar between PD and GWL. Lower GWL resulted in higher PD. Those comparable results indicate that GWL mostly can be used as a proxy for PD, even at different land uses and sites.

Not only affecting PD, GWL was also found to influence the variation of peat elevation both in rubber and oil palm plantations (Chapters 2 and 4). Therefore, to determine the peat subsidence correctly, peat elevation should be measured simultaneously with GWL measurement. Using BD and C content, annual subsidence resulting from oxidative peat decomposition was calculated to be 1.50 and 2.33 cm yr^{-1} in rubber and oil palm plantations, respectively. BD and C content in rubber plantation were 0.23 and 42.8 %, whereas in oil palm plantation were 0.14 g cm^{-3} and 48.1%. The rates of subsidence were in parallel to PD in both sites though the BD and C content were different. Higher PD resulted in higher subsidence.

To separate RR and directly measure PD, a trenching approach was used in the rubber plantation (Chapter 2). In oil palm plantation, however, PD was measured far from tree rows (about 3 m from tree bases; Chapter 4). We confirmed that SR was significantly larger than PD both in rubber and oil palm plantations. Despite the fact that the trenching approach has limitations and shortcomings (Epron, 2009; Hanson et al., 2000; Subke et al., 2006), we found that this approach was effective to measure PD separately because RR in the rubber plantation was observed not to decrease with a distance from tree bases. SR in the rubber plantation was not significantly different between at near and far positions from tree rows (Chapter 2). In the oil palm plantation, however, RR decreased with a distance from tree bases. SR in oil palm plantation was declined progressively with the increasing distance from each oil palm tree base (Chapter 4), which is consistent with those of previous studies (Dariah et al., 2014; Ishikura et al., 2018; Manning, 2019).

This study also established the contribution of CO_2 emission through pruned frond decomposition (LD_{frond}) in oil palm plantations (Chapters 3 and 4). This is the

first study to estimate the LD_{frond}. Therefore, HR that defined as a sum of PD and LD_{frond} could be estimated (Chapter 4). However, no comparison result was found, because most of the existing studies did not clearly yet separated the emission result from PD and HR from various land uses in forest or plantations.

5.2. Carbon sequestration through net primary production (NPP)

Not only emission, this study also showed the C sequestration through NPP in oil palm plantations. The highest NPP was recorded in the industrial plantation in Riau (17.3 Mg C ha^{-1} yr^{-1}), followed by smallholder plantations in Jambi (13.5 Mg C ha^{-1} yr^{-1}) and South Kalimantan (10.9 Mg C ha^{-1} yr^{-1}). In all sites, total NPP was mostly contributed from ANPP in the range of 73 to 81% from total NPP (Chapter 3 and 4).

Total NPP was influenced by the age of plantation as indicated by the higher NPP of mature plantations in Riau and Jambi than that of a young plantation in South Kalimantan. Also, NPP was affected by management, in which industrial plantation tends to have higher NPP than that of smallholder plantation, as shown by higher NPP in industrial plantation in Riau than that of smallholder plantation in Jambi. Furthermore, yield production of industrial plantation was higher than smallholder plantation in Indonesia (Directorate general of estate crops, Indonesia Ministry of Agriculture, 2017). Industrial plantations generally have better cultivation management, whereas smallholder plantations often have problems arising from inadequate knowledge in cultivation, the use of counterfeit seed, and insufficient fertilizer application, which result in their lower yields (Vermeulen and Goad, 2006; Woittiez et al., 2017). Besides, poor yields in smallholder plantations in Jambi and South Kalimantan were likely supported by the lack of proper water management on peat soil, which requires drainage canals or flood gates. However, these proper canal or flood gates are usually cannot be implemented in the smallholder plantations due to the lower income.

5.3. Carbon balance of agricultural plantations on peat soil

Direct measurements of two contrast fluxes, soil CO_2 emission through peat decomposition (PD) including CO_2 emission through pruned frond decomposition (LD_{frond}) and carbon sequestration through NPP in this study allow us to show the C balance of rubber and oil palm plantations in Indonesia's tropical peatland (Table 20). C balance is defined as a balance between C sequestration through NPP and CO_2 emission through HR. Due to the limitation of data, we used some results from previous studies for a better comparison in both plantations. For rubber plantation in Central Kalimantan, we used NPP of 15.4 Mg C ha^{-1} yr^{-1} from rubber plantation on

mineral soil in Jambi (Kotowska et al., 2015). Also, in rubber plantation, C input through litter fall of 1.88 Mg C ha^{-1} yr^{-1} (Kotowska et al., 2016) was used for C emission through rubber leaf decomposition (LD_{rubber}) with an assumption that the litter fall was all decomposed in a year. For oil palm plantation in Riau, we used PD of 12.2 Mg C ha^{-1} yr^{-1} from 14 years old of industrial oil palm plantation that measured near our site (Marwanto et al., 2019). Whereas in Jambi, we used PD of 9.30 Mg C ha^{-1} yr^{-1} from 15 years old of smallholder oil palm plantations in the same province (Dariah et al., 2014). As a result, a young oil palm plantation in South Kalimantan and rubber plantation in Central Kalimantan were estimated as a C source. Oil palm plantation in South Kalimantan was a C source possibility due to the lower NPP because of the plantation immaturity. Therefore, the C balance in South Kalimantan might be different in the following years as the oil palm trees growing to mature.

Table 20. C balance calculated as the difference of annual C input through net primary production (NPP) and CO_2 emission through heterotrophic soil respiration (HR), as a sum of peat decomposition (PD) and litter decomposition (LD). LD consists of litter decomposition from pruned frond (LD_{frond}) and litter decomposition from rubber leaf (LD_{rubber}).

Plantation	C input through NPP (Mg C ha^{-1} yr^{-1})	C emission	Mg C ha^{-1} yr^{-1}	C Balance (Mg C ha^{-1} yr^{-1})
Rubber in Central Kalimantan	15.4	PD	14.1	-0.56
		LD_{rubber}	1.88	
		HR	16.0	
Young oil palm in South Kalimantan	10.9	PD	15.4	-4.86
		LD_{frond}	0.38	
		HR	15.8	
Mature oil palm in Riau	17.3	PD	12.2	3.61
		LD_{frond}	1.48	
		HR	13.7	
Mature (old) oil palm in Jambi	13.5	PD	9.30	3.08
		LD_{frond}	1.12	
		HR	10.4	

5.4. Implications for tropical peat management

Lower GWL, which results in a higher PD, mostly happens due to drainage in plantations. In contrast, this drainage is needed to sustain the optimal growth of plantation commodities. Therefore, a better understanding of appropriate GWL to

suppress PD and meet the ideal condition for plantation growth is essential. On the other hand, soil temperature was found to affect PD mostly in the open area (Melling et al., 2013; Jauhiainen et al., 2014; Hergoualc'h et al., 2017; Manning et al., 2019). Sparse canopies of land allowing direct sunlight to reach and warm the peat soil surface. Therefore, studying how to increase the shading of peat soil surface on plantations is needed, particularly on young plantations. Not only as shading, the cover crop is also planted to support the production of main crop, as we found in the intercropping system in a rubber plantation in Central Kalimantan (Chapter 2) and understory vegetation in an oil palm plantation in Riau (Chapter 3).

To reduce the emission, some researchers suggest to maintain GWL high and lowering the soil temperature by peat shading. In application, however, maintaining GWL high was difficult, because hydrological conditions are complex in peat (Ritzema et al., 2014). Along with emission reduction, another alternative is to increase C sequestration through NPP. Applying a better management, such as using certified seed, good soil tillage, and effective fertilizer, would increase the yield of agricultural plantations production, and simultaneously, raise the C sequestration.

Chapter 6. Conclusions

Two carbon fluxes, namely soil CO_2 emissions including CO_2 emission through pruned frond decomposition (LD_{frond}) and C sequestration through net primary production (NPP) were investigated in two major land uses on peat soil in Indonesia, rubber and oil palm plantations.

First, in a rubber plantation, in Central Kalimantan, soil CO_2 efflux through oxidative peat decomposition (PD) was measured using chamber method in trenching plots during 2015, a strong El Niño year. PD showed a clear seasonality and linearly increased as groundwater level (GWL) decreased. Using the strong linearity, annual PD was estimated from continuous GWL data to be 14.1 Mg C ha^{-1} yr^{-1}. However, the annual PD was determined in a strong El Niño year with drought. Thus, in a normal year without El Niño drought or in a La Niña year, annual PD in the rubber plantation most probably reduces in proportion to GWL. Similarly, the linear relationship indicates that annual PD can be simply assessed from only mean annual GWL. Also, the seasonal variation of peat elevation was showed in parallel with GWL. The parallel variation indicates that GWL should be considered carefully to determine peat subsidence for assessing PD using the subsidence method.

Second, in mature oil palms, an industrial plantation in Riau and a smallholder plantation in Jambi, Sumatra, annual NPP and LD_{frond} were directly measured from February 2018 to July 2019. In both plantations, total NPP was dominated by aboveground NPP, of which the most contribution was from fruit production. In belowground NPP, contribution of fine root was much higher than that of coarse root, suggesting that fine root NPP should be treated as an important source of NPP in oil palm plantations. Also, understory vegetation should be counted for NPP. Total NPP was estimated to be 17.3 and 13.5 Mg C ha^{-1} yr^{-1}, in Riau and Jambi, respectively. Total NPP of industrial plantation in Riau was higher than that of smallholder plantation in Jambi, which suggests difference in plantation management influenced NPP. Not only C sequestration through NPP, LD_{frond} was also higher in Riau.

Third, in a young smallholder oil palm plantation in South Kalimantan, annual PD, LD_{frond}, and NPP were measured from September 2018 to March 2020. PD showed a significant negative linear relationship with GWL even with the low coefficient of determination. As a sum of PD (15.4) and LD_{frond} (0.38) Mg C ha^{-1} yr^{-1}, heterotrophic respiration (HR) was estimated to be 15.8 Mg C ha^{-1} yr^{-1}. On the other side, NPP was dominated by aboveground NPP. However, as a young plantation that still produces a

small amount of fruit, the most contribution to NPP was from tree canopy production. Total NPP was estimated to be 10.9 Mg C ha^{-1} yr^{-1}. The low NPP in this site mostly due to the plantation immaturity. Therefore, this plantation was estimated to be a CO_2 source of -4.86 Mg C ha^{-1} yr^{-1} as a result of C balance between NPP and HR.

References

Afriyanti, D., Kroeze, C., Saad, A., 2016. Indonesia palm oil production without deforestation and peat conversion by 2050. Science of Total Environment 557-558: 562–570. http://doi.org/10.1016/j.scitotenv.2016.03.032.

Aguilos, M., Takagi, K., Liang, N., Watanabe, Y., Teramoto, M., Goto, S., Takahashi, Y., Mukai, H., Sasa, K., 2013. Sustained large stimulation of soil heterotrophic respiration rate and its temperature sensitivity by soil warming in a cool-temperate forested peatland. Tellus B 65: 20792. http://doi.org/10.3402/tellusb.v65i0.20792.

Agus, F., Hairiah, K., Mulyani, A., 2011. Measuring carbon stock in peat soils: practical guidelines. World Agroforestry Centre (ICRAF) Southeast Asia Regional Program. Indonesian Centre for Agricultural Land Resources Research and Development, Bogor, Indonesia.

Agus, F., Gunarso, P., Sahardjo, B.H., Harris, N., Noordwijk, M.V., Killeen, T.J., 2013. Historical CO_2 emissions from land use and land use change from the oil palm industry in Indonesia, Malaysia and Papua New Guinea. Reports from the Technical Panels of the 2nd Greenhouse Gas Working Group of the Roundtable on Sustainable Palm Oil (RSPO). Tropenbos International.

Ali, M., Taylor, D., Inubushi, K., 2006. Effects of environmental variations on CO_2 efflux from a tropical peatland in eastern Sumatra. Wetlands 26: 612–618. http://doi.org/10.1672/0277-5212(2006)26[612:EOEVOC]2.0.CO;2.

An, J., Y., Park, B., B., Chun, J., H., Osawa, A., 2017. Litterfall production and fine root dynamics in cool-temperate forests. PLoS ONE 12 (6): 1-16. http://doi.org/10.1371/journal.pone.0180126.

Basuki, I., Kauffman, J.B., Peterson, J., Anshari, G., and Murdiyarso, D., 2018. Land cover changes reduce net primary production in tropical coastal peatlands of West Kalimantan, Indonesia. Mitigation and Adaptation Strategies for Global Change 24 (4): 557–573. http://doi.org/10.1007/s11027-018-9811-2.

BPS-Statistics Indonesia, 2019. Estates Area by Crops, Indonesia (000 Ha), 1995 - 2018. https://www.bps.go.id. Accessed May 30, 2020.

BPS-Statistics of Riau Province, 2019. Riau Province in figures 2019. BPS-Statistics of Riau Province. Riau, Indonesia.

BPS-Statistics of Tanjung Jabung Timur Regency, 2019. Tanjung Jabung Timur Regency in figures. BPS-Statistics of Tanjung Jabung Timur Regency. Jambi, Indonesia.

Bragazza, L., Buttler, A., Siegenthaler, A., and Mitchell, E.A.D., 2008. Plant litter decomposition and nutrient release in peatlands. Carbon Cycling in Northern Peatlands (Geophysical Monograph Series) 184: 99-110.

Carlson, K.M., Curran, L., Asner, G., Pittman, A., Trigg, S., Adeney, J., 2012. Carbon emissions from forest conversion by Kalimantan oil palm plantations. Nature Climate Change 3 (3): 283-287. http://doi.org/10.1038/nclimate1702.

Carlson, K.M., Goodman, L.K., May-Tobin, C.C., 2015. Modeling relationships between water table depth and peat soil carbon loss in Southeast Asian plantations. Environmental Research Letter 10: 074006. http://doi.org/10.1088/1748-9326/10/7/074006.

Chimner, R.A., and Ewel, K.C., 2005. A tropical freshwater wetland: II. Production, decomposition, and peat formation. Wetlands Ecology and Management 13: 671–684. http://doi.org/10.1007/s11273-005-0965-9.

Clark, D., Brown, S., Kicklighter, D., Chambers, J., Thomlinson, J., Ni, J., Holland, E., 2001. Net primary production in tropical forests: an evaluation and synthesis of existing field data. Ecological Applications 11 (3): 944-944. http://doi.org/10.1890/1051-0761(2001)011[0371:NPPITF]2.0.CO;2.

Comeau, L.P., Hergoualc'h, K., Smith, J., Verchot, L.V., 2013. Conversion of intact peat swamp forest to oil palm plantation: effects on soil CO_2 fluxes in Jambi, Sumatra. Working Paper 110. Indonesia, CIFOR, Bogor.

Comeau, L.P., Hergoualc'h, K., Hartill, J., Smith, J., Verchot, L.V., Peak, D., Salim, A.M., 2016. How do the heterotrophic and the total soil respiration of an oil palm plantation on peat respond to nitrogen fertilizer application? Geoderma. 268: 41–51. http://doi.org/10.1016/j.geoderma.2016.01.016.

Corley, R.H.V., and Tinker, P.B., 2003. The Oil Palm, Fourth Edition. Blackwell Science Ltd, UK.

Couwenberg, J., Dommain, R., Joosten, H., 2009. Greenhouse gas fluxes from tropical peatlands in South-east Asia. Global Change Biology 16: 1715–1732. http://doi.org/10.1111/j.1365-2486.2009.02016.x.

Couwenberg, J., and Hooijer, A., 2013. Towards robust subsidence-based soil carbon emission factors for peat soils in South-east Asia, with special reference to oil palm plantations. Mires and Peat 12: 1–13.

Dariah, A., Marwanto, S., Agus, F., 2014. Root- and peat-based CO_2 emissions from oil palm plantations. Mitig. Adapt. Strateg. Glob. Chang. 19: 831–843. http://doi.org/10.1007/s11027-013-9515-6.

Directorate General of Estate Crops, Indonesia Ministry of Agriculture, 2017. Tree crop estate statistics of Indonesia 2016-2018, palm oil. Secretariat of Directorate General of Estate Crops. Ministry of Agriculture. Jakarta, Indonesia.

Epron, D., 2009. Separating autotrophic and heterotrophic components of soil respiration; lessons learned from trenching and related root-exclusion experiments. 157–168. In: Kutsch, W.L., Bahn, M., Heinemeyer, A. (Eds.), Soil Carbon Dynamics 2009. Cambridge University Press, New York, p. 286.

FAOSTAT (Food and Agriculture Organization of the United Nations Statistics Division), 2014. Crops processed; Indonesia and World list; Oil, palm; Production quantity; 2014. http://faostat3.fao.org/download/Q/QD (accessed 21 October 2019).

Finér, L., Ohashi, M., Noguchi, K., Hirano, Y., 2011. Fine root production and turnover in forest ecosystems in relation to stand and environmental characteristics. Forest Ecology and Management 262 (11): 2008-2023. http://doi.org/10.1016/j.foreco.2011.08.042.

Furukawa, Y., Inubushi, K., Ali, M., Itang, A.M., Tsuruta, H., 2005. Effect of changing groundwater levels caused by land-use changes on greenhouse gas fluxes from tropical peatlands. Nutr. Cycl. Agroecosyst 71: 81–91.

Gill, R.A., and Jackson, R.B., 2000. Global patterns of root turnover for terrestrial ecosystems. New Phytologist 147: 13-31. http://doi.org/10.1046/j.1469-8137.2000.00681.x.

Global Business Guide Indonesia, 2015. Indonesia's Global Business Guide Indonesia, 2015. Indonesia's Downstream Rubber Industry–Waiting for Investors. https://www.gbgindonesia.com/en/agriculture/article. Accessed September 9, 2016.

Gunarso, P., Hartoyo, M.E., Agus, F., and Killeen, T.J., 2013. Oil palm and land use change in Indonesia, Malaysia and Papua New Guinea, in: Killeen, T.J. and Goon, J. (Eds.), Reports from the Technical Panels of the Second RSPO GHG Working Group, Roundtable for Sustainable Palm Oil – RSPO, Kuala Lumpur, Malaysia.

Hanson, P.J., Edwards, N.T., Garten, C.T., Andrews, J.A., 2000. Separating root and soil microbial contributions to soil respiration: a review of methods and observations. Biogeochemistry 48: 115–146.

Harazono, Y., Iwata, H., Sakabe, A., Ueyama, M., Takahashi, K., Nagano, H., Nakai, T., Kosugi, Y., 2015. Effects of water vapor dilution on trace gas flux, and practical correction methods. J. Agric. Meteorol. 71: 65–76. http://doi.org/10.2480/agrmet.D-14-00003.

Henson, I.E., 2017. A review of models for assessing carbon stocks and carbon sequestration in oil palm plantations. Journal of oil palm research 29 (1): 1-10. http://doi.org/10.21894/jopr.2017.2901.01.

Hergoualc'h, K., Verchot, L.V., 2011. Stocks and fluxes of carbon associated with land use change in Southeast Asian tropical peatlands: a review. Glob. Biogeochem. Cycles 25: GB2001. http://doi.org/10.1029/2009GB003718.

Hergoualc'h, K., Verchot, L.V., 2013. Greenhouse gas emission factors for land use and land-use change in Southeast Asian peatlands. Mitig. Adapt. Strateg. Glob. Chang. 19: 789–807. http://doi.org/10.1007/s11027-013-9511-x.

Hergoualc'h, K., Hendry, D. T., Murdiyarso, D., and Verchot, L. V., 2017. Total and heterotrophic soil respiration in a swamp forest and oil palm plantations on peat in Central Kalimantan, Indonesia. Biogeochemistry 135: 203–220. http://doi.org/10.1007/s10533-017-0363-4.

Hirano, T., Jauhiainen, J., Inoue, T., Takahashi, H., 2009. Controls on the carbon balance of tropical peatlands. Ecosystems 12: 873–887. http://doi.org/10.1007/s10021-008- 9209-1.

Hirano, T., Kusin, K., Limin, S., Osaki, M., 2014. Carbon dioxide emissions through oxidative peat decomposition on a burnt tropical peatland. Glob. Chang. Biol. 20: 555–565. http://doi.org/10.1111/gcb.12296.

Hirano, T., Kusin, K., Limin, S., Osaki, M., 2015. Evapotranspiration of tropical peat forests. Glob. Chang. Biol. 21: 1914–1927. http://doi.org/10.1111/gcb.12653.

Hooijer, A., Page, S., Canadell, J.G., Silvius, M., Kwadijk, J., Wösten, H., Jauhiainen, J., 2010. Current and future CO_2 emissions from drained peatlands in Southeast Asia. Biogeosciences 7: 1505–1514. http://doi.org/10.5194/bg-7-1505-2010.

Hooijer, A., Page, S., Jauhiainen, J., Lee, W.A., Lu, X.X., Idris, A., Anshari, G., 2012. Subsidence and carbon loss in drained tropical peatlands. Biogeosciences 9: 1053–1071. http://doi.org/10.5194/bg-9-1053-2012.

Hooijer, A., Page, S., Navratil, P., Vernimmen, R., Van der Vat, M., Tansey, K., Konecny, K., Siegert, F., Ballhorn, U., Mawdsley, N., 2014. Carbon emissions from drained and degraded peatland in Indonesia and emission factors for measurement, reporting and verification (MRV) of peatland greenhouse gas

emissions - a summary of KFCP research results for practitioners. IAFCP, Jakarta, Indonesia.
Husen, E., Salma, S., Agus, F., 2014. Peat emission control by groundwater management and soil amendments: evidence from laboratory experiments. Mitig. Adapt. Strateg. Glob. Chang. 19: 821–829. http://doi.org/10.1007/s11027-013-9526-3.
Husnain, H., Wigena, I.G.P., Dariah, A., Marwanto, S., Setyanto, P., Agus, F., 2014. CO_2 emissions from tropical drained peat in Sumatra, Indonesia. Mitig. Adapt. Strateg. Glob. Chang. 19:845–862. http://doi.org/10.1007/s11027-014-9550-y.
Huxman, T.E., Snyder, K.A., Tissue, D., Leffler, A.J., Ogle, K., Pockman, W.T., Sandquist, D.R., Potts, D.L., 2004. Precipitation pulses and carbon fluxes in semiarid and arid ecosystems. Oecologia 141:254–268. http://doi.org/10.1007/s00442-004-1682-4.
Iiyama, I., Osawa, K., 2010. Surface O_2 in flux related to soil O_2 profiles in a drained tropical peatland. Soil Sci. Plant Nutr. 56:517–520. http://doi.org/10.1111/j.1747-0765.2010.00488.x.
IPCC, 2014. 2013 Supplement to the 2006 IPCC Guidelines for National Greenhouse Gas Inventories. IPCC, Wetlands, Switzerland.
Inubushi, K., Furakawa, Y., Hadi, A., Purnomo, E., Tsuruta, H., 2003. Seasonal change of CO_2, CH_4 and N_2O fluxes in relation to land-use change in tropical peatlands located in coastal area of South Kalimantan. Chemosphere 52:603–608. http://doi.org/10.1016/S0045-6535(03)00242-x.
Ishikura, K., Yamada, H., Toma, Y., Takakai, F., Morishita, T., Darung, U., Limin, A., Limin, S.H., Hatano, R., 2016. Effect of groundwater level fluctuation on soil respiration rate of tropical peatland in Central Kalimantan, Indonesia. Soil Science and Plant Nutrition 63 (1): 1–13. http://doi.org/10.1080/00380768.2016.1244652.
Ishikura, K., Hirano, T., Okimoto, Y., Hirata, R., Kiew, F., Melling, L., Aeries, E.B.; Lo, K.S., Musin, K.K., Waili, J.W., Wong G. X., Ishii Y., 2018. Soil carbon dioxide emissions due to oxidative peat decomposition in an oil palm plantation on tropical peat. Agriculture, Ecosystem and Environment 254: 202–212. http://doi.org/10.1016/j.agee.2017.11.025.
Itoh, M., Kosugi, Y., Takanashi, S., Kanemitsu, S., Osaka, K., Hayashi, Y., Tani, M., Rahim, A.N., 2012. Effects of soil water status on the spatial variation of carbon dioxide, methane and nitrous oxide fluxes in tropical rain-forest soils in peninsular Malaysia. J. Trop. Ecol. 28: 557–570. http://doi.org/10.1017/S0266467412000569.
Itoh, M., Okimoto, Y., Hirano, T., Kusin, K., 2017. Factors affecting oxidative peat decomposition due to land use in tropical peat swamp forests in Indonesia. Sci. Total Environ. 609: 906–915. http://doi.org/10.1016/j.scitotenv.2017.07.132.
Jauhiainen, J., Takahashi, H., Heikkinen, J.E.P., Martikainen, P.J., Vasanderet, H., 2005. Carbon fluxes from a tropical peat swamp forest floor. Glob. Chang. Biol. 11:1788–1797. http://doi.org/10.1111/j.1365-2486.2005.001031.x.
Jauhiainen, J., Hooijer, A., Page, S.E., 2012. Carbon dioxide emissions from an Acacia plantation on peatland in Sumatra, Indonesia. Biogeosciences 9:617–630. http://doi.org/10.5194/bg-9-617-2012.
Jauhiainen, J., Kerojoki, O., Silvennoinen, H., Limin, S., Vasander, H., 2014. Heterotrophic respiration in drained tropical peat is greatly affected by

temperature-a passive ecosystem cooling experiment. Environ. Res. Lett. 9:105013. http://doi.org/10.1088/1748-9326/9/10/105013.
Jourdan, C., and Rey, H., 1997. Architecture and development of the oil palm (Elaeis guineensis Jacq.) root system. Plant and Soil 189: 33–48.
Khalid, H., Zin, Z.Z., Anderson, J.M., 2000. Decomposition processes and nutrient release patterns of oil palm residues. Journal of Oil Palm Research 12 (1): 46-63.
Kharina, A., Malins, C., and Searle, S., 2016. Biofuels policy in Indonesia: Overview and status report, White Paper. International Council on Clean Transportation, Washington DC.
Khasanah, N., van Noordwijk, M., Ningsih, H., 2015. Aboveground carbon stocks in oil palm plantations and the threshold for carbon-neutral vegetation conversion on mineral soils. Cogent Environmental Science 1. http://doi.org/10.1080/23311843.2015.1119964.
Khasanah, N., and van Noordwijk, M., 2018. Subsidence and carbon dioxide emissions in a smallholder peatland mosaic in Sumatra, Indonesia. Mitigation and Adaptation Strategies for Global Change volume 24:147–163. http://doi.org/10.1007/s11027-018-9803-2.
Koh, L., Miettinen, J., Liew, S., Ghazoul, J., 2011. Remotely sensed evidence of tropical peatland conversion to oil palm. Proc. Natl. Acad. Sci. USA. http://doi.org/10.1073/pnas.1018776108.
Könönen, M., Jauhiainen, J., Laiho, R., Kusin, K., Vasander, H., 2015. Physical and chemical properties of tropical peat under stabilised land uses. Mires and Peat 16: 1–13.
Kotowska, M.M., Leuschner, C., Triadiati, T., Selis, M., Hertel, D., 2015. Quantifying above- and belowground biomass carbon loss with forest conversion in tropical lowlands of Sumatra (Indonesia). Global Change Biology 21: 3620–3634. http://doi.org/10.1111/gcb.12979.
Kotowska, M.M., Leuschner, C., Triadiati, T., Hertel, D., 2016. Conversion of tropical lowland forest reduces nutrient return through litterfall and alters nutrient use efficiency and seasonality of net primary production. Oecologia 180: 601–618. http://doi.org/10.1007/s00442-015-3481-5.
Kwon, M.J., Haraguchi, A., Kang, H., 2013. Long-term water regime differentiates changes in decomposition and microbial properties in tropical peat soils exposed to the short-term drought. Soil Biol. Biochem. 60: 33–44. http://doi.org/10.1016/j.soilbio.2013. 01.023.
Lamade, E., and Bouillet, J.P., 2005. Carbon storage and global change: the role of oil palm. Oléagineux Corps Gras Lipides (OCL) 12: 154–160. http://doi.org/10.1051/ocl.2005.0154.
Lee, X., Wu, H.-J., Sigler, J., Oishi, C., Siccama, T., 2004. Rapid and transient response of soil respiration to rain. Glob. Chang. Biol. 10: 1017–1026. http://doi.org/10.1111/j.1365-2486.2004.00787.x
Leuschner, C., Harteveld, M., Hertel, D., 2009. Consequences of increasing forest use intensity for biomass, morphology and growth of fine roots in a tropical moist forest on Sulawesi, Indonesia. Agricultural, Ecosystem and Environment 129: 474–481. http://doi.org/10.1016/j.agee.2008.10.023.
Maeght, J.L., Gonkhamdee, S., Clément, C., Ayuttaya, S.I.N., Stokes, A., Pierret, A., 2015. Seasonal patterns of fine root production and turnover in a mature rubber

tree (Hevea brasiliensis Müll. Arg.) stand differentiation with soil depth and implications for soil carbon stocks. Front. Plant Sci. 6:1022. http://doi.org/10.3389/fpls.2015.01022.

Majdi, H., and öhrvik, J., 2004. Interactive effects of soil warming and fertilization on root production, mortality, and longevity in a Norway spruce stand in Northern Sweden. Global Change Biology 10: 182-188. http://doi.org/10.1111/j.1365-2486.2004.00733.x.

Makkonen, K., and Helmisaari, H.S., 1999. Assessing fine-root biomass and production in a Scots pine stand-comparison of soil core and root ingrowth core methods. Plant and Soil 210: 43-50. http://doi.org/10.1023/A:1004629212604.

Manning, F., C., Kho, L., K., Hill, T., C., Cornulier, T., and Teh, Y., A., 2019. Carbon emissions from oil palm plantations on peat soil. Front. For. Glob. Change 2:37. http://doi.org/10.3389/ffgc.2019.00037.

Marchante, E., Kjøller, A., Struwe, S., Freitas, H., 2008. Short- and long-term impacts of *Acacia longifolia* invasion on the belowground processes of a Mediterranean coastal dune ecosystem. Appl. Soil Ecol. 40:210–217. http://doi.org/10.1016/j.apsoil. 2008.04.004.

Marwanto, S., Agus, F., 2014. Is CO_2 flux from oil palm plantations on peatland controlled by soil moisture and/or soil and air temperatures? Mitig. Adapt. Strateg. Glob. Chang. 19:809–819. http://doi.org/10.1007/s11027-013-9518-3.

Marwanto, S., Sabiham, S., Funakawa, S., 2019. Importance of CO_2 production in subsoil layers of drained tropical peatland under mature oil palm plantation. Soil and Tillage Research. 186: 206-213. http://doi.org/10.1016/j.still.2018.10.021.

Matsuura, S., Mori, A., Hojito, M., Kanno, T., Sasaki, H., 2011. Evaluation of a portable chamber system for soil co2 efflux measurement and the potential errors caused by internal compensation and water vapor dilution. J. Agric. Meteorol. 67:123–137.

Melling, L., Hatano, R., Goh, K.J., 2005. Soil CO_2 flux from three ecosystems in tropical peatland of Sarawak, Malaysia. Tellus 57B: 1–11.

Melling, L., Goh, K.J., Beauvais, C., Hatano, R., 2008. Carbon flow and budget in a young mature oil palm agroecosystem on deep tropical peat. The planter 84 (982): 21–25.

Melling, L., Yun Tan, C.S., Goh, K.J., Hatano, R., 2013. Soil microbial and root respirations from three ecosystems in tropical peatland of Sarawak, Malaysia. J. Oil Palm Res. 25: 44–57.

Miettinen, J., Hooijer, A., Shi, C., Tollenaar, D., Vernimmen, R., Liew, S.C., Malins, C., Page, S.E., 2012. Extent of industrial plantations on Southeast Asian peatlands in 2010 with analysis of historical expansion and future projections. GCB Bioenergy 4: 908–918. http://doi.org/10.1111/j.1757-1707.2012.01172.x.

Miettinen, J., Shi, C., Liew, S.C., 2016. Land cover distribution in the peatlands of peninsular Malaysia, Sumatra and Borneo in 2015 with changes since 1990. Global Ecology and Conservation 6:67–78. http://doi.org/10.1016/j.gecco.2016.02.004.

Miyamoto, K., Kohyama, T.S., Rahajoe, J.S., Mirmanto, E., Simbolon, H., 2016. Forest structure and productivity of tropical heath and peatland forests, in: Osaki, M., Noboyuki, T. (Eds.), Tropical peatland ecosystems. Springer. pp. 151–166.

Moradi, A., Teh C.B.S., Goh, K.J., Husni, M.H.A., Ishak, C.F., 2013. Decomposition and nutrient release temporal pattern of oil palm residues. Annals of Applied Biology 164 (2): 208-219. http://doi.org/10.1111/aab.12094.

Murayama, S., Bakar, Z.A., 1996a. Estimation of in situ decomposition by measurement of CO_2 flux. JARQ30, 153–158.

Murayama, S., Bakar, Z.A., 1996b. Decomposition kinetics of organic matter of peat soils. JARQ30 145–151.

Nagano, T., Osawa, K., Ishida, T., Sakai, K., Vijarnsorn, P., Jongskul, A., 2013. Subsidence and soil CO_2 efflux in tropical peatland in southern Thailand under various water table and management conditions. Mires and Peat 11: 1–20.

Nakano, T., Sawamoto, T., Morishita, T., Inoue, G., Hatano, R., 2004. A comparison of regression methods for estimating soil atmosphere diffusion gas fluxes by a closed chamber technique. Soil Biol. Biochem. 36: 107–113. http://doi.org/10.1016/j.soilbio.2003.07.005.

Nurzakiah, S., Sabiham, S., Nugroho, B., Nursyamsi, D., 2014. Estimation of the potential carbon emission from acrotelmic and catotelmic peats. J. Tropical Soil 19: 91–99.

Page, S.E., Siegert, F., Rieley, J.O., Boehm, H.V., Jaya, A., Limin, S.H., 2002. The amount of carbon released from peat and forest fires in Indonesia during 1997. Nature 420: 61–65.

Page, S.E., Rieley, J.O., Banks, C.J., 2011a. Global and regional importance of the tropical peatland carbon pool. Glob. Chang. Biol. 17:798–818. http://doi.org/10.1111/j. 1365-2486.2010.02279.x.

Page, S.E., Morrison, R., Malins, C., Hooijer, A., Rieley, J.O., Jauhiainen, J., 2011b. Review of peat surface greenhouse gas emissions from oil palm plantations in Southeast Asia. White Paper Number 15Indirect Effects of Biofuel Production Series. International Council on Clean Transportation Funding, Washington DC.

Pathiratna, 2006. Management of intercrops under rubber: implications of competition and possibilities for improvement. Bull. Rubber Res. Inst. Sri Lanka 47: 8–16.

Pauli, N., Donough, C., Oberthür, T., Cock, J., Verdooren, R., Rahmadsyah, Abdurrohim, G., Indrasuara, K., Lubis, A., Dolong, T., Pasuquin, J.M., 2014. Changes in soil quality indicators under oil palm plantations following application of 'best management practices' in a four-year field trial. Agriculture, Ecosystems and Environment 195:98-111. http://doi.org/10.1016/j.agee.2014.05.005.

Pirker, J., Mosnier, A., Kraxner, F., Havlík, P., Obersteiner, M., 2016. What are the limits to oil palm expansion? Global Environmental Change 40:73–81. http://doi.org/10.1016/j.gloenvcha.2016.06.007.

Ritzema, H., Limin, S., Kusin, K., Jauhiainen, J., Wösten, H., 2014. Canal blocking strategies for hydrological restoration of degraded tropical peatlands in Central Kalimantan, Indonesia. Catena 114: 11–20. http://doi.org/10.1016/j.catena.2013.10.009.

Safitri, L., Hermantoro, H., Purboseno, S., Kautsar, V., Saptomo, S.K., Kurniawan, A., 2019. Water footprint and crop water usage of oil palm (*Eleasis guineensis*) in Central Kalimantan: Environmental sustainability indicators for different crop age and soil conditions. Water 11: 35. http://doi.org/10.3390/w11010035.

Sakata, R., Shimada, S., Arai, H., Yoshioka, N., Yoshioka, R., Aoki, H., Kimoto, N., Sakamoto, A., Melling, L., Inubushi, K., 2015. Effect of soil types and nitrogen fertilizer on nitrous oxide and carbon dioxide emissions in oil palm plantations. Soil Science and Plant Nutrition 61: 48–60. http://doi.org/10.1080/00380768.2014.960355.

Saragi-Sasmito, M., F., Murdiyarso, D., June, T., Sasmito, S., D., 2018. Carbon stocks, emissions, and aboveground productivity in restored secondary tropical peat swamp forests. Mitigation and Adaptation Strategies for Global Change 1–13. http://doi.org/ 10.1007/s11027-018-9793-0.

Schiermeier, Q., 2015. Hunting the Godzilla El Niño. Nature 526: 490–491.

Schrier-Uijl, A., P., Silvius, M., Parish, F., Lim, K., H., Rosediana, S., Anshari, G., 2013. Environmental and social impacts of oil palm cultivation on tropical peat – a scientific review. Round table on Sustainable Palm Oil (Kuala Lumpur, Malaysia).

Scurlock, J.M.O., Johnson, K., Olson, R.J., 2002. Estimating net primary productivity from grassland biomass dynamic measurements. Global Change Biology 8: 736-753. http://doi.org/10.1046/j.1365-2486.2002.00512.x.

Shimada, S., Takahashi, H., Haraguchi, A., Kaneko, M., 2001. The carbon content characteristics of tropical peats in Central Kalimantan, Indonesia: estimating their spatial variability in density. Biogeochemistry 53: 249–267. http://doi.org/10.1023/A:1010618807469.

Subke, J.A., Inglima, I., Cotrufo, M.F., 2006. Trends and methodological impacts in soil CO_2 efflux partitioning: a meta analytical review. Glob. Chang. Biol. 12: 1–23. http://doi. org/10.1111/j.1365-2486.2006.01117.x.

Sundari, S., Hirano, T., Yamada, H., Kusin, K., Limin, S., 2012. Effects of groundwater level on soil respiration in tropical peat swamp forests. J. Agric. Meteorol. 68: 121–134. http://doi.org/10.2480/agrmet.68.2.6.

Syahrinudin, 2005. The potential of oil palm and forest plantations for carbon sequestration on degraded land in Indonesia, Ecology and Development Series 28. Cuvillier Verlag, G€ottingen.

Tan, K.P., Kanniah, K.D., Cracknell A.P., 2014. On the upstream inputs into the MODIS primary productivity products using biometric data from oil palm plantations. International Journal of Remote Sensing 35 (6): 2215-2246. http://doi.org/10.1080/01431161.2014.889865.

Violita, Triadiati, Anas, I., Miftahudin, 2016. Fine root production and decomposition in lowland rainforest and oil palm plantations in Sumatra, Indonesia. Hayati Journal of Biosciences 23 (1): 7-12. http://doi.org/10.1016/j.hjb.2015.10.008.

Verheye, W., 2010. Growth and production of rubber. In: Verheye, W. (Ed.), Land Use, Land Cover and Soil Sciences. Encyclopedia of Life Support Systems (EOLSS). UNESCO-EOLSS Publishers, Oxford, UK.

Vermeulen, S., and Goad, N., 2006. Towards better practice in smallholder palm oil production, Natural Resource Issues Series No. 5. International Institute for Environment and Development, London, UK.

Wahyunto, N., K., Ritung, S., Sulaeman, Y., 2014. Indonesian peatland map: method, certainty, and uses. Indonesian Center for Agroclimate Research and Development, Indonesian Agency for Agricultural Research and Development, Ministry of Agriculture, Jakarta, Indonesia.

Wosten, J.H.M., 1997. Peat subsidence and its practical implications: a case study in Malaysia. Geoderma 78: 25–36.

Woittiez, L., S.,van Wijk, M., T., Slingerland, M., van Noordwijk, M., 2017. Yield gaps in oil palm: A quantitative review of contributing factors. European Journal of Agronomy 83: 57–77. http://doi.org/10.1016/j.eja.2016.11.002.

Yuan, Z. Y., and Chen, H.Y.H., 2012. Indirect methods produce higher estimates of fine root production and turnover rates than direct methods. PLoS ONE 7(11): e48989. http://doi.org/ 10.1371/journal.pone.0048989.

Yuan, Z.Y., and Chen, H.Y.H., 2013. Simplifying the decision matrix for estimating fine root production by the sequential soil coring approach. Acta Oecologica. 48, 54-61. http://doi.org/10.1016/j.actao.2013.01.009.

Yuen, J.Q., Ziegler, A.D., Webb, E.L., Ryan, C.M., 2013. Uncertainty in below-ground carbon biomass for major land covers in South-east Asia. Forest Ecology Management 310: 915–926. http://doi.org/10.1016/j. foreco.2013.09.042.